

Crustal Deformation

Takeshi Sagiya

Disaster Mitigation Research Center

Nagoya University

(E-mail: sagiya@nagoya-u.jp)

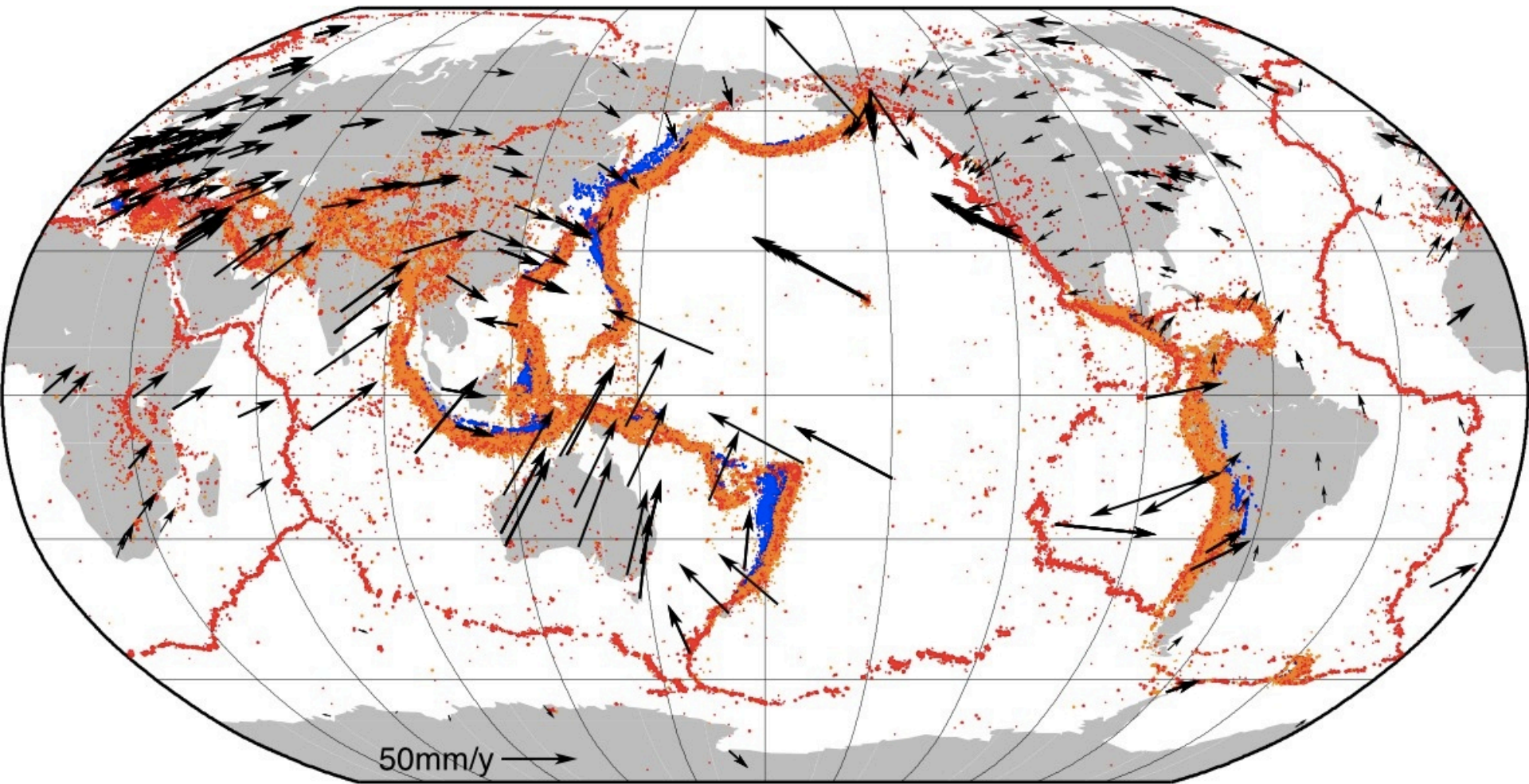
Contents

- Introduction
- Theory of crustal deformation
- Observation methods
- Earthquake deformation
- Volcano deformation

1. Introduction

- Importance of crustal deformation
 - Tectonics
 - Plate motions to understand regional tectonics
 - Earthquake/Tsunami
 - Strain accumulation to investigate seismogenic potential
 - Deformation associated with earthquakes to investigate size and mechanism of an earthquake and to predict tsunami
 - Postseismic deformation to reveal rheological/frictional properties
 - Precursory deformation to predict earthquakes
 - Volcano
 - Magmatic inflation under a volcano to investigate potential for future eruption
 - Monitor magmatic motion during eruption activity

Global seismicity and crustal motion

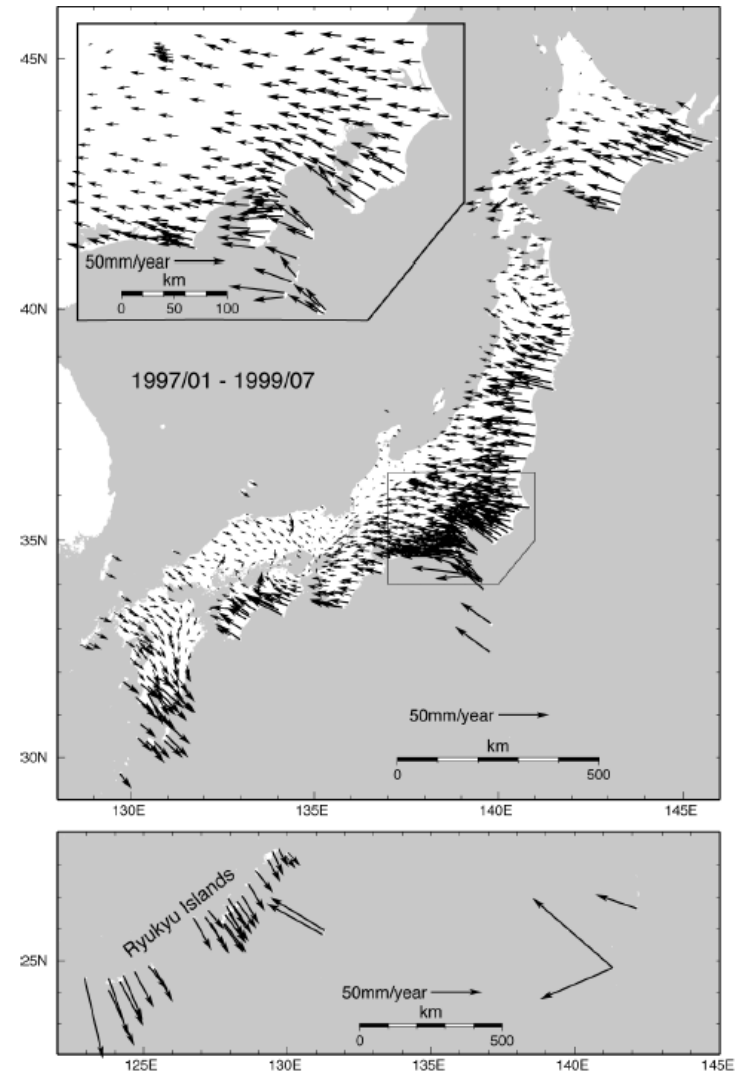
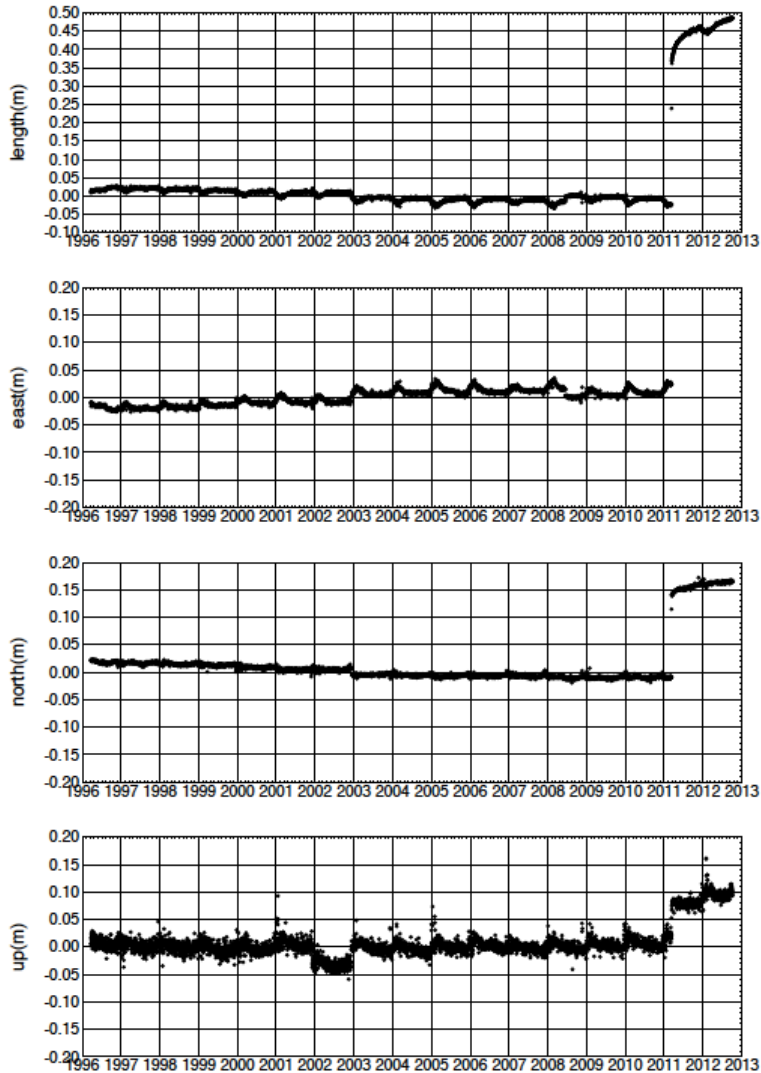


Seismicity: USGS catalogue (1973-2009), $M > 5$
GPS: ITRF2005 solution

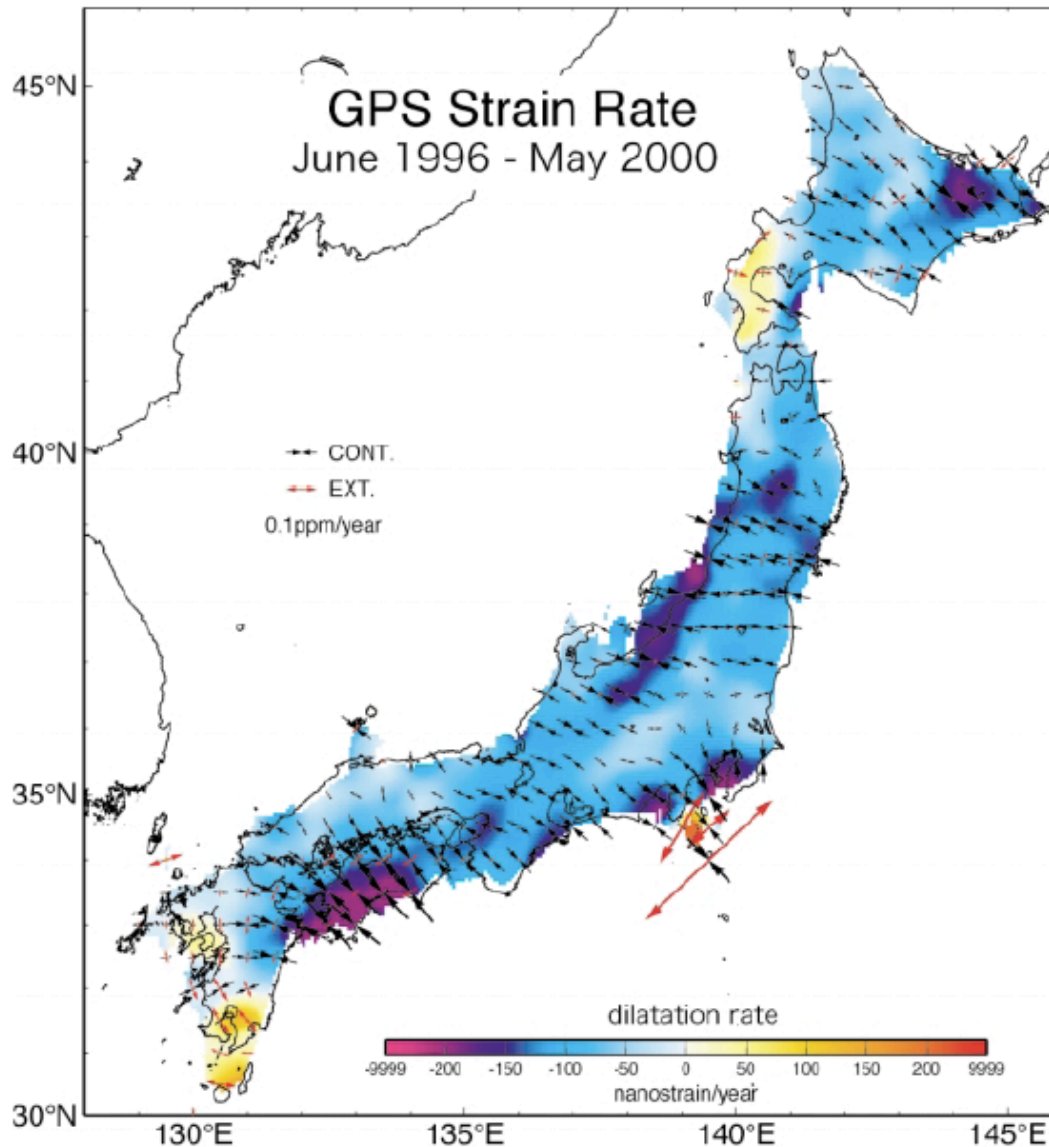
Example: GPS data

Horizontal velocity

Coordinate time series

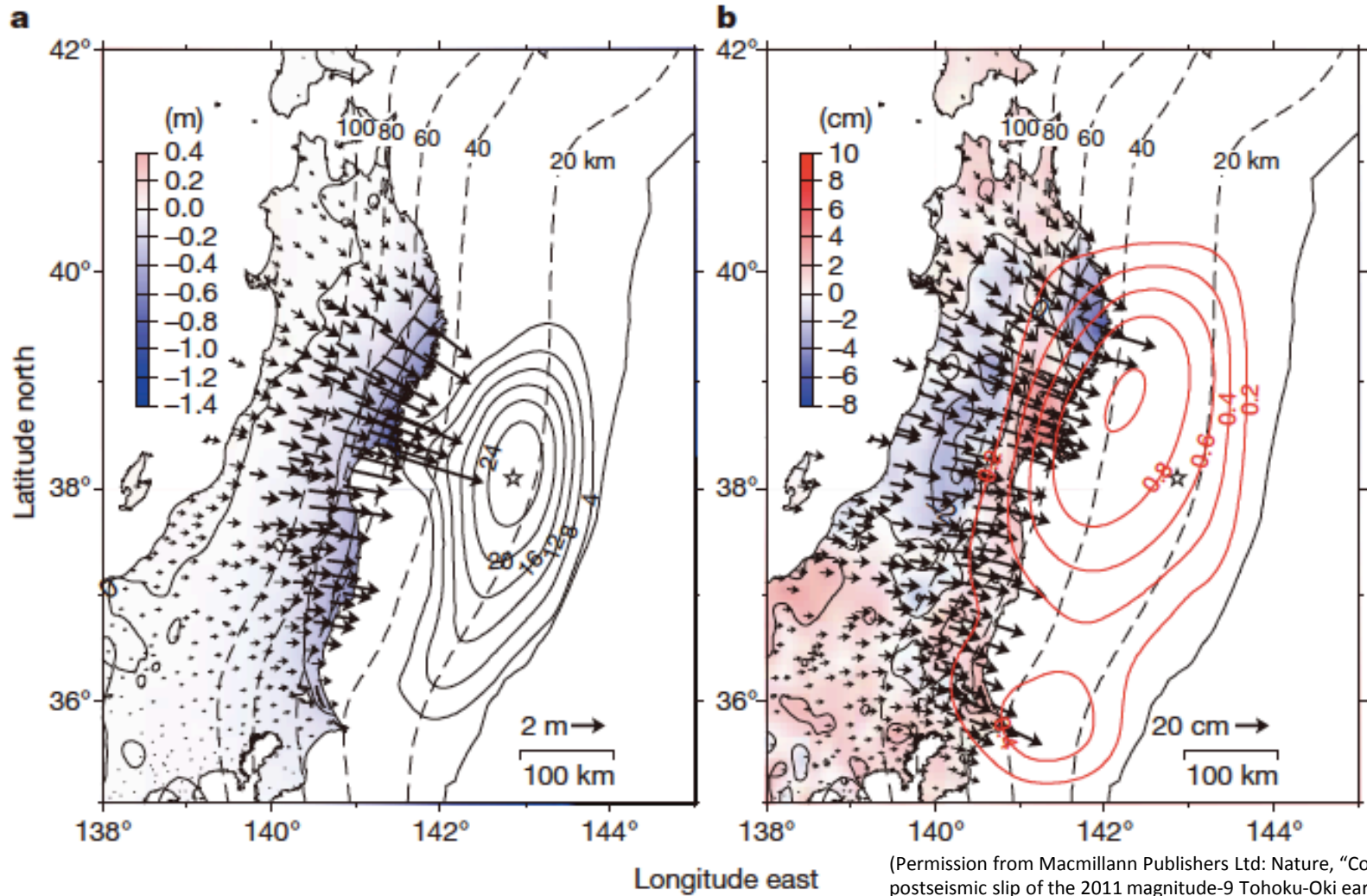


Strain rate distribution



(Sagiya, T., A decade of GEONET: 1994-2003
"The continuous GPS observation in Japan and
its impact on earthquake studies",
Earth Planets Space, 56, xxix-xli, 2004.)

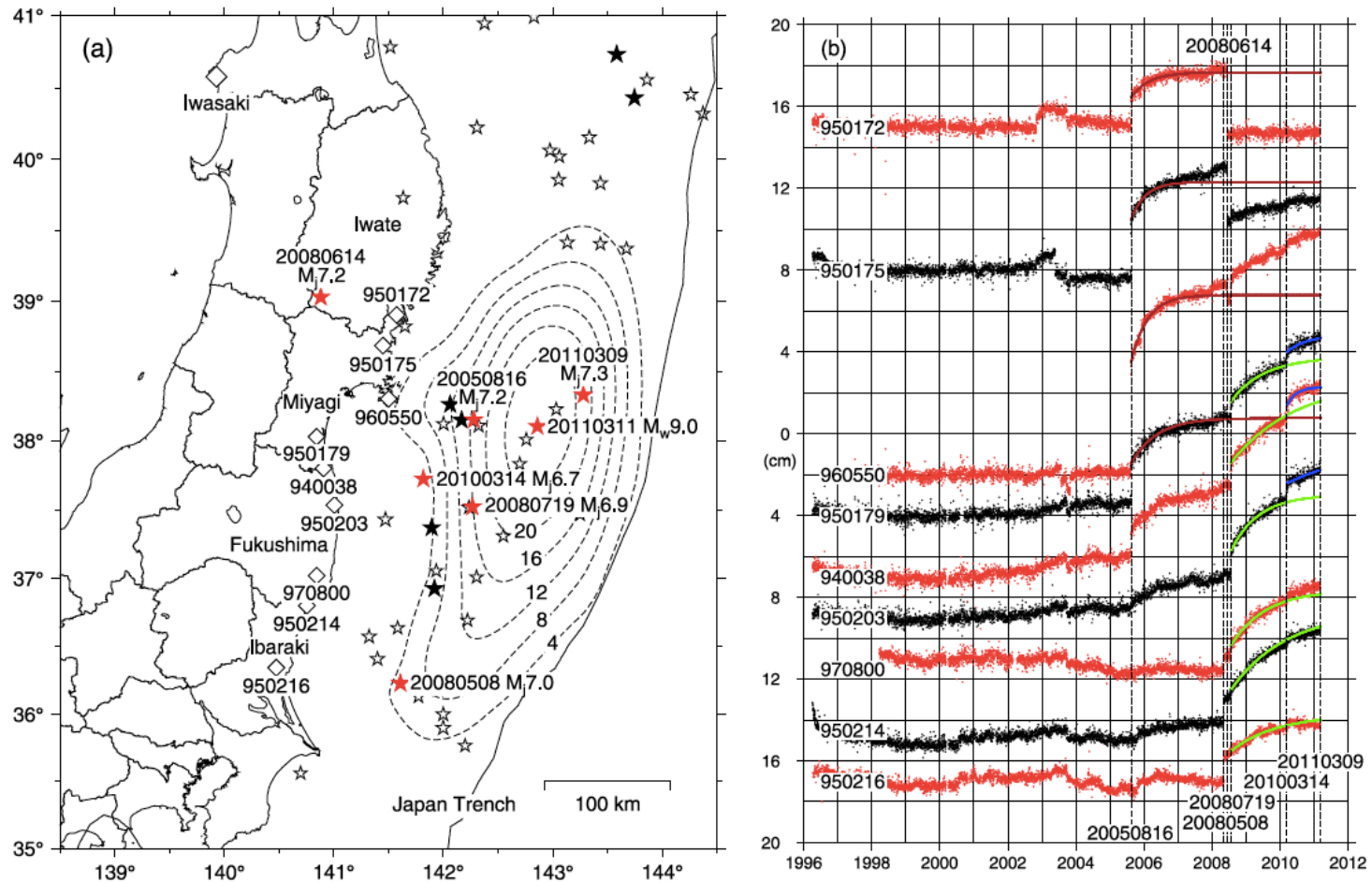
Coseismic and postseismic deformation



(Permission from Macmillann Publishers Ltd: Nature, "Coseismic and postseismic slip of the 2011 magnitude-9 Tohoku-Oki earthquake", Ozawa et al., 2011)

The 2011 Tohoku-Oki Earthquake (M9.0)

Precursory deformation?

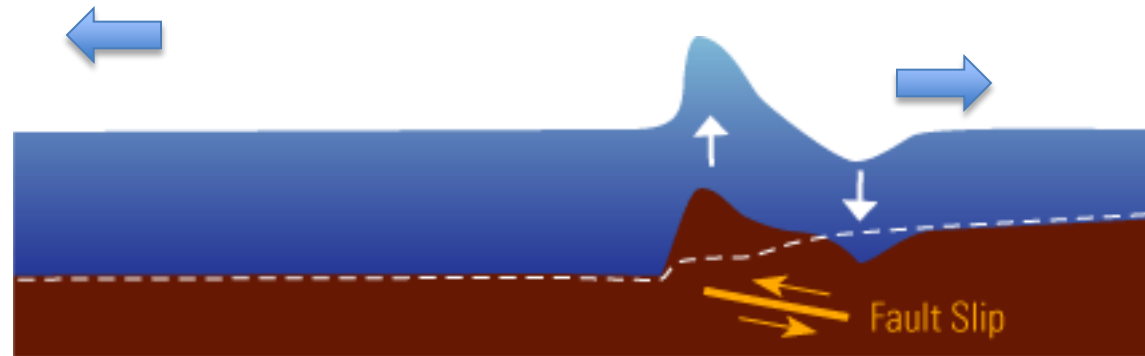


Short-term precursor was not evident, but the displacement seems to have accelerating for several years before the main shock.

(Suito et al., "Interplate fault slip along the Japan Trench before the occurrence of the 2011 off the Pacific coast of Tohoku Earthquake as inferred from GPS data", Earth Planets Space, 63, 615-619, 2011.)

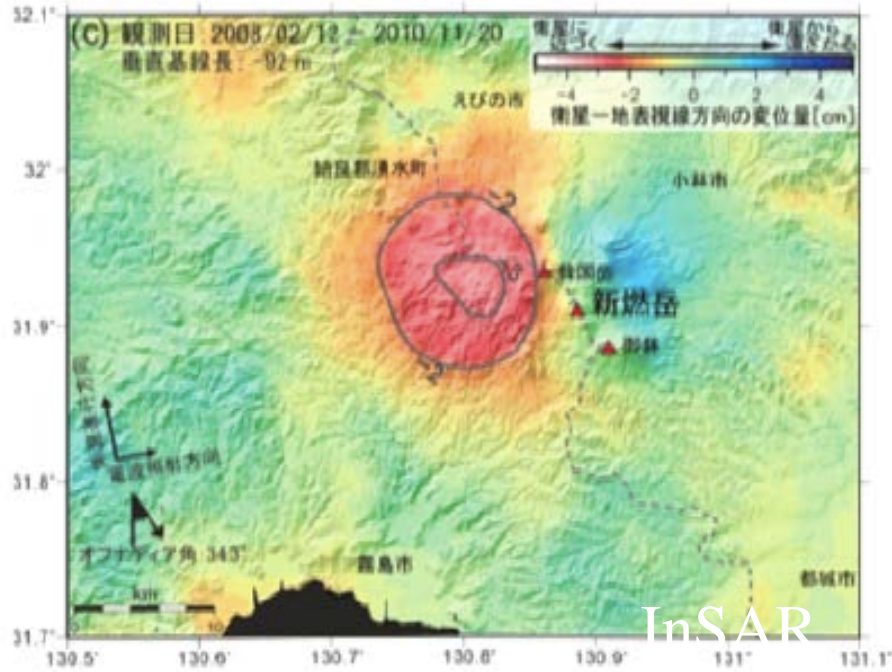
Tsunami

- Tsunami is caused by crustal deformation at the seafloor.
- Coseismic uplift/subsidence of coastal area may affect tsunami inundation.
- Appropriate modeling of offshore crustal deformation is indispensable for successful tsunami prediction and warning.



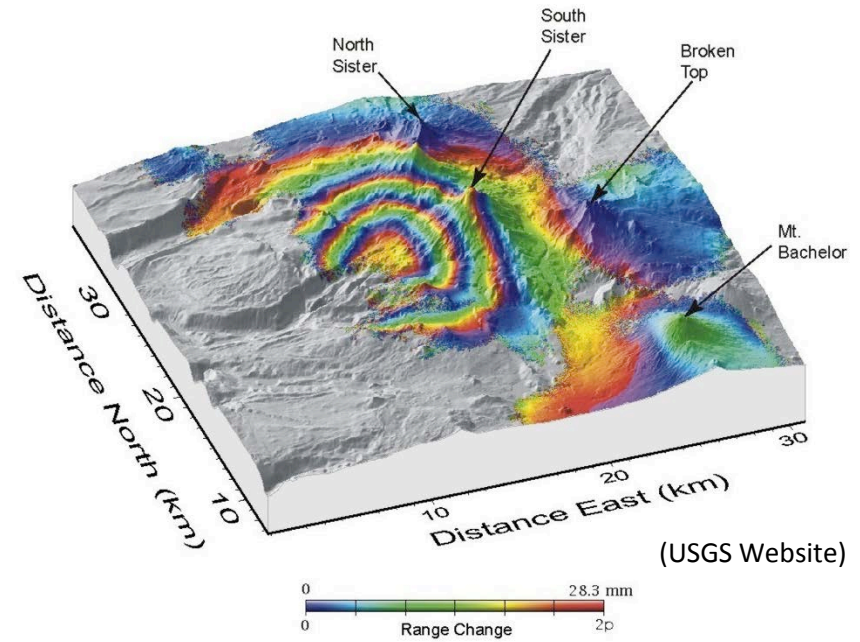
Volcano deformation in a dormant period

Kirishima



InSAR

Three sisters, Oregon

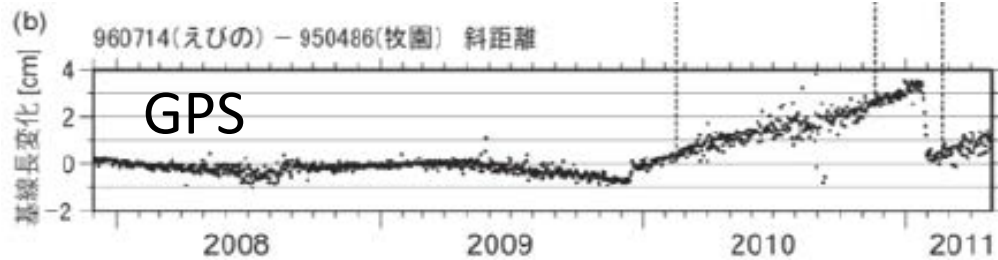


(USGS Website)

0 28.3 mm
0 Range Change 2p
GMT May 1 10:43 Interferogram by C Wicks, USGS

USGS

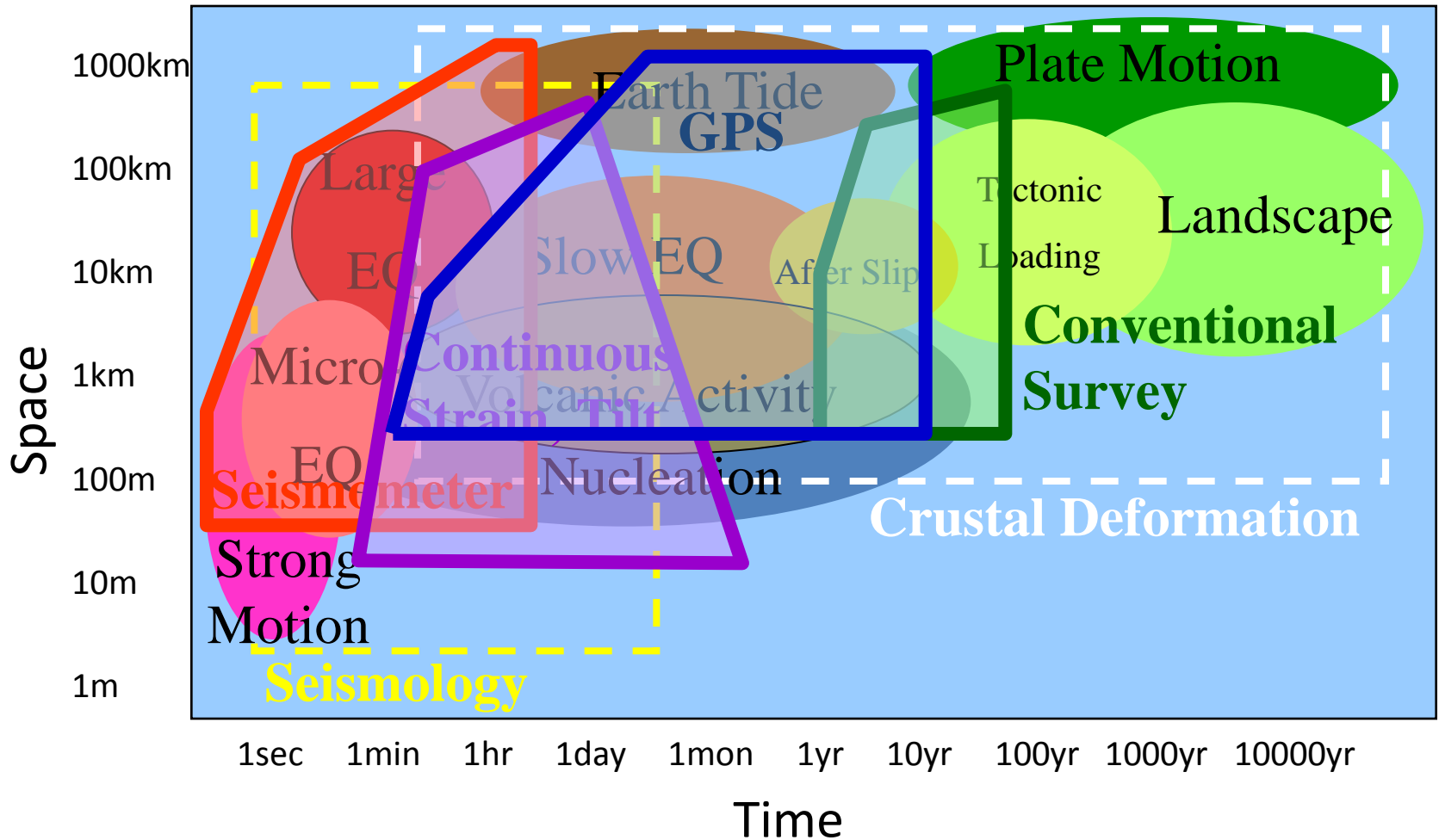
- Detection of uplift due to magmatic inflation
- Deformation is a key for volcano monitoring



GPS

(Kobayashi et al., 2011, GSI Website: <http://www.gsi.go.jp/common/000062664.pdf>)

Spatio-temporal range of observations



2. Theory of crustal deformation

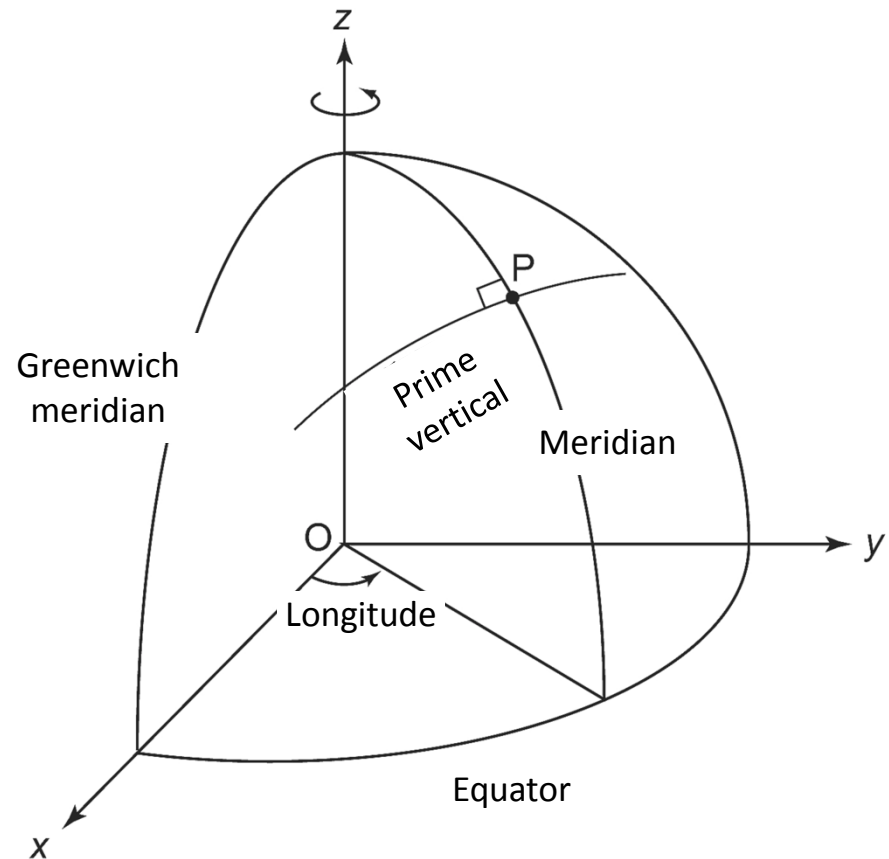
- Reference frame
- Displacement and displacement rate
- Strain and strain rate
- Tilt
- Stress and strain

2.1. Reference frame

- Crustal deformation is measured in a reference frame
- Global reference frame
 - (Latitude, Longitude, Height)
 - (X, Y, Z) : geocentric coordinate
- Local reference frame
 - (East, North, Up)

2.1 Reference frame

- Geocentric coordinate system
 - Origin: center of mass
 - X-axis: intersection of the Greenwich meridian and the equatorial plane
 - Y-axis: intersection of the 90° E meridian and the equatorial plane
 - Z-axis: direction of the North pole
 - Independent of ellipsoid

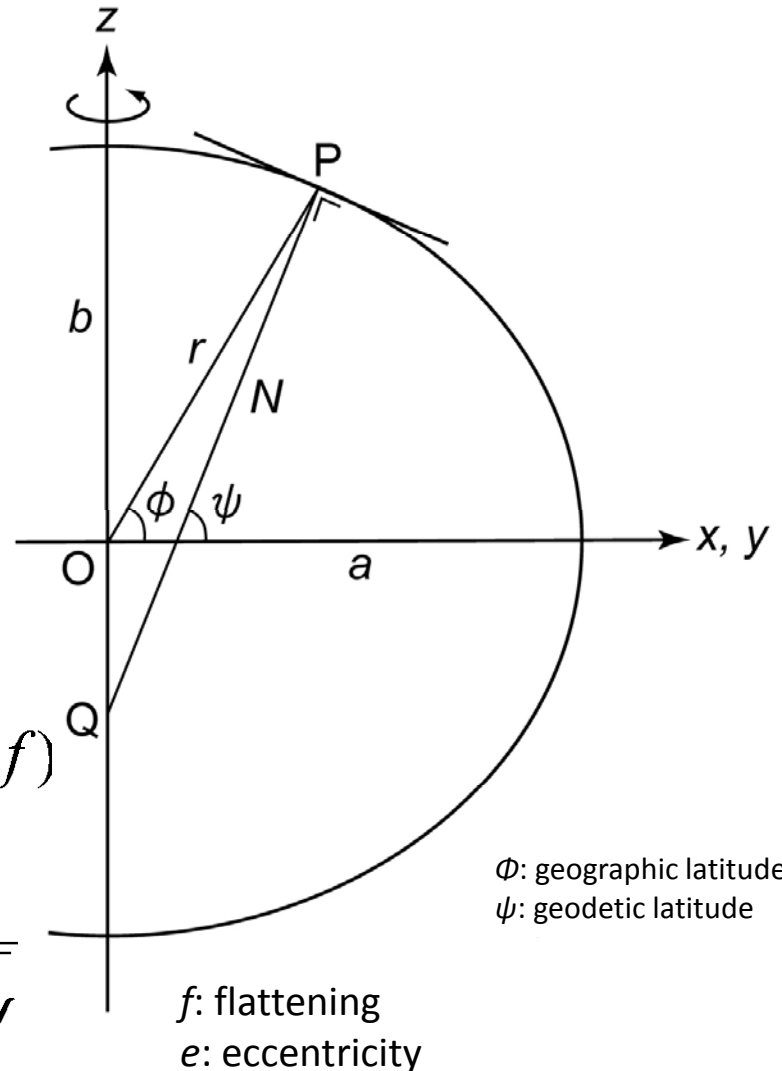


2.1 Reference frame

- Ellipsoid is a good approximation of the shape of the Earth
- GRS80 Ellipsoid
 - $a=6,378,137\text{m}$
 - $f=1/298.257$

$$\frac{x^2 + y^2}{a^2} + \frac{z^2}{b^2} = 1 \quad f = \frac{a-b}{a} \quad e^2 = f(2-f)$$

$$r = \frac{b}{\sqrt{1 - e^2 \sin^2 \phi}} \quad N = \frac{a}{\sqrt{1 - e^2 \sin^2 \psi}}$$



Transformation formula

$$(\psi, \lambda, H) \rightarrow xyz$$

ψ : Latitude (geodetic)

λ : Longitude

H : Ellipsoidal height

$$x = (N + H) \cos \psi \cos \lambda$$

$$y = (N + H) \cos \psi \sin \lambda$$

$$z = \left(N \frac{b^2}{a^2} + H \right) \sin \psi$$

$$xyz \rightarrow (\psi, \lambda, H)$$

$$\lambda = \tan^{-1} \left(\frac{x}{y} \right)$$

$$\psi_0 = \tan^{-1} \left(\frac{z}{\sqrt{x^2 + y^2}} \right)$$

$$N_i = \frac{a}{\sqrt{1 - e^2 \sin^2 \psi_i}}$$

$$\psi_{i+1} = \tan^{-1} \left(\frac{z + N_i e^2 \sin \psi_i}{\sqrt{x^2 + y^2}} \right)$$

$$H = \frac{\sqrt{x^2 + y^2}}{\cos \psi} - N$$

Transformation formula

- To transform coordinate change in global reference frame into local coordinate system

$$\begin{pmatrix} dE \\ dN \\ dU \end{pmatrix} = \begin{pmatrix} -\sin\lambda & \cos\lambda & 0 \\ -\sin\varphi \cos\lambda & -\sin\varphi \sin\lambda & \cos\varphi \\ \cos\varphi \cos\lambda & \cos\varphi \sin\lambda & \sin\varphi \end{pmatrix} \begin{pmatrix} dx \\ dy \\ dz \end{pmatrix}$$

2.1 Reference frame

- How can we define precise positions on the incessantly deformation Earth?
- Only relative motions between sites are available from observations.
- Currently adopted reference frames (ITRF, International Terrestrial Reference Frame) are realized by applying no-net-translation and no-net-rotation condition to the observation data.
- Current model: ITRF2008 (Altamimi et al., 2011)
 - <http://itrf.ensg.ign.fr/>
 - Defined by precise coordinates and their change rates at geodetic network sites

ITRF2008

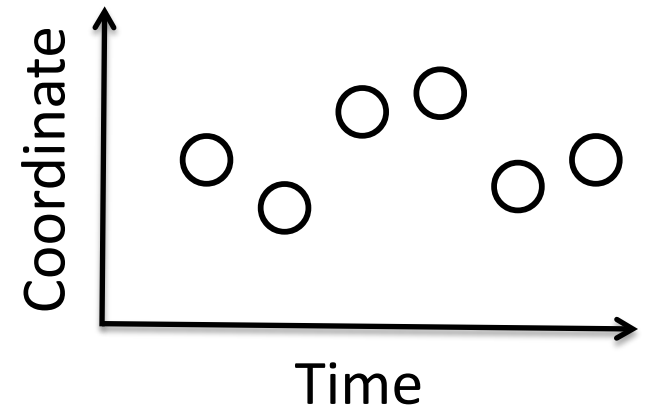
ITRF2008 STATION POSITIONS AT EPOCH 2005.0 AND VELOCITIES IGS STATIONS

DOMES NB.	SITE NAME	TECH. ID.	X/Vx	Y/Vy	Z/Vz	Sigmatas	SOLN	DATA_START	DATA_END
			-----m/m/y-----						
10001S006	Paris	GNSS OPMT	4202777.371	171367.999	4778660.203	0.001	0.001	0.001	
10001S006			-.0125	0.0178	0.0107	.0001	.0000	.0001	
10002M006	Grasse (OCA)	GNSS GRAS	4581690.901	556114.831	4389360.793	0.001	0.001	0.001	1 00:000:00000 03:113:00000
10002M006			-.0133	0.0188	0.0120	.0001	.0000	.0001	
10002M006	Grasse (OCA)	GNSS GRAS	4581690.900	556114.837	4389360.793	0.001	0.001	0.001	2 03:113:00000 04:295:43200
10002M006			-.0133	0.0188	0.0120	.0001	.0000	.0001	
10002M006	Grasse (OCA)	GNSS GRAS	4581690.900	556114.836	4389360.797	0.001	0.001	0.001	3 04:295:43200 00:000:00000
10002M006			-.0133	0.0188	0.0120	.0001	.0000	.0001	
10003M004	Toulouse	GNSS TOUL	4627846.029	119629.333	4372999.818	0.001	0.001	0.001	
10003M004			-.0114	0.0193	0.0121	.0001	.0000	.0001	
10003M009	Toulouse	GNSS TLSE	4627851.831	119640.017	4372993.553	0.001	0.001	0.001	1 00:000:00000 03:335:00000
10003M009			-.0114	0.0193	0.0121	.0001	.0000	.0001	
10003M009	Toulouse	GNSS TLSE	4627851.828	119640.020	4372993.552	0.001	0.001	0.001	2 03:335:00000 00:000:00000
10003M009			-.0114	0.0193	0.0121	.0001	.0000	.0001	

(ITRF, http://itrf.ensg.ign.fr/ITRF_solutions/2008/doc/ITRF2008_GNSS.SSC.txt)

2.2 Displacement and displacement rate

- “Displacement” is defined as a coordinate change from one time to another time.
- Observed daily coordinates always contain observational errors.
- To describe displacements, mentioning their value as well as their errors is indispensable.
- Root-mean-square is a measure representing repeatability of coordinates, and is a good measure of observational errors.



$$RMS = \sqrt{\frac{1}{n} \sum_{i=1}^n (x_i - \bar{x})^2}$$

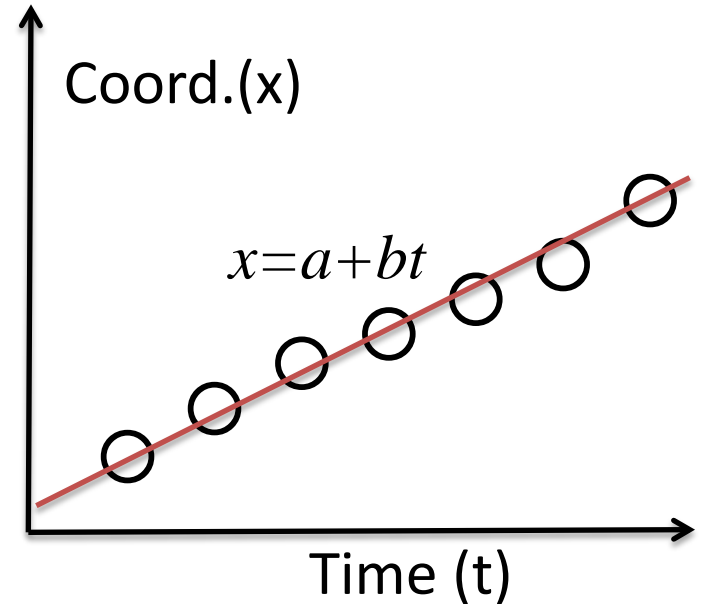
$$\bar{x} = \frac{1}{n} \sum_{i=1}^n x_i$$

2.2 Displacement and displacement rate

- In order to detect significant crustal displacement, observations should be made:
 - Over a long enough time (for large enough displacement to accumulate)
 - With good measurement technology (to be capable of small coordinate change)
- Interpretation of displacement data needs special attention since they contain effects of rigid block translation, rigid rotation, and strain (deformation).

2.2 Displacement and displacement rate

- When we have long enough coordinate time series data and they exhibit a steady change, we can calculate displacement rate.
- Least squares method is applied for calculation of displacement rate.



$$x_i = a + bt_i$$

2.2 Displacement and displacement rate

- Least squares method
 - Minimize sum of squared normalized residuals
 - Normalized residual using data error σ_i .

$$S = \sum_{i=1}^n \left\{ \frac{x_i - (a + bt_i)}{\sigma_i} \right\}^2$$

$$\frac{\partial S}{\partial a} = -2 \sum_{i=1}^n \frac{x_i - (a + bt_i)}{\sigma_i^2} = 0$$

$$\frac{\partial S}{\partial b} = -2 \sum_{i=1}^n \frac{t_i \{x_i - (a + bt_i)\}}{\sigma_i^2} = 0$$

$$\begin{bmatrix} \sum_{i=1}^n \frac{1}{\sigma_i^2} & \sum_{i=1}^n \frac{t_i}{\sigma_i^2} \\ \sum_{i=1}^n \frac{t_i}{\sigma_i^2} & \sum_{i=1}^n \frac{t_i^2}{\sigma_i^2} \end{bmatrix} \begin{bmatrix} a \\ b \end{bmatrix} = \begin{bmatrix} \sum_{i=1}^n \frac{x_i}{\sigma_i^2} \\ \sum_{i=1}^n \frac{t_i x_i}{\sigma_i^2} \end{bmatrix}$$

2.2 Displacement and displacement rate

- Seasonal component
 - Coordinate time series often show seasonal variation.
 - These variations are either natural (e.g. snow load) or artificial (e.g. erroneous tropospheric model).
 - Seasonal components can be corrected by applying an appropriate observational equation.

$$x_i = a + bt_i + c \sin 2\pi t_i + d \cos 2\pi t_i$$

$$\begin{bmatrix} x_1 \\ x_2 \\ \vdots \\ x_n \end{bmatrix} = \begin{bmatrix} 1 & t_1 & \sin 2\pi t_1 & \cos 2\pi t_1 \\ 1 & t_2 & \sin 2\pi t_2 & \cos 2\pi t_2 \\ \vdots & \vdots & \vdots & \vdots \\ 1 & t_n & \sin 2\pi t_n & \cos 2\pi t_n \end{bmatrix} \begin{bmatrix} a \\ b \\ c \\ d \end{bmatrix}$$

$$\mathbf{x} = \mathbf{H}\mathbf{m}$$

$$\mathbf{H}^t \mathbf{x} = \mathbf{H}^t \mathbf{H} \mathbf{m}$$

$$\mathbf{m} = (\mathbf{H}^t \mathbf{H})^{-1} \mathbf{H}^t \mathbf{x}$$

More complicated case:

$$x_i = a + bt_i + \sum_{j=1}^N \{c_j \sin 2\pi j t_i + d_j \cos 2\pi j t_i\}$$

2.3 Strain and strain rate

- Strain describes deformation of continuum (solid and fluid)
- Displacement contains information of strain, rigid translation, and rigid rotation
- Strain components are defined as spatial derivatives of displacement. Infinitesimal strain (Cauchy's strain) is defined as:

$$\varepsilon_{ij} = \frac{1}{2} \left(\frac{\partial u_j}{\partial x_i} + \frac{\partial u_i}{\partial x_j} \right)$$

- When deformation is not infinitesimal, different definition of finite strain should be used
- Strain is dimensionless.
- Strain rate is strain change per unit time, or spatial derivative of velocity.

2.3 Strain and strain rate

- 2-D case: Taylor expansion of displacement

$$u = u_0 + \frac{\partial u}{\partial x}x + \frac{\partial u}{\partial y}y = \boxed{u_0} + \boxed{\frac{\partial u}{\partial x}}x + \boxed{\frac{1}{2}\left(\frac{\partial u}{\partial y} + \frac{\partial v}{\partial x}\right)}y + \boxed{\frac{1}{2}\left(\frac{\partial v}{\partial x} - \frac{\partial u}{\partial y}\right)}y$$

$$v = v_0 + \frac{\partial v}{\partial x}x + \frac{\partial v}{\partial y}y = \boxed{v_0} + \boxed{\frac{1}{2}\left(\frac{\partial u}{\partial y} + \frac{\partial v}{\partial x}\right)}x + \boxed{\frac{\partial v}{\partial y}}y + \boxed{\frac{1}{2}\left(\frac{\partial v}{\partial x} - \frac{\partial u}{\partial y}\right)}x$$

– Rigid translation

$$\boxed{(u_0, v_0)}$$

– Strain

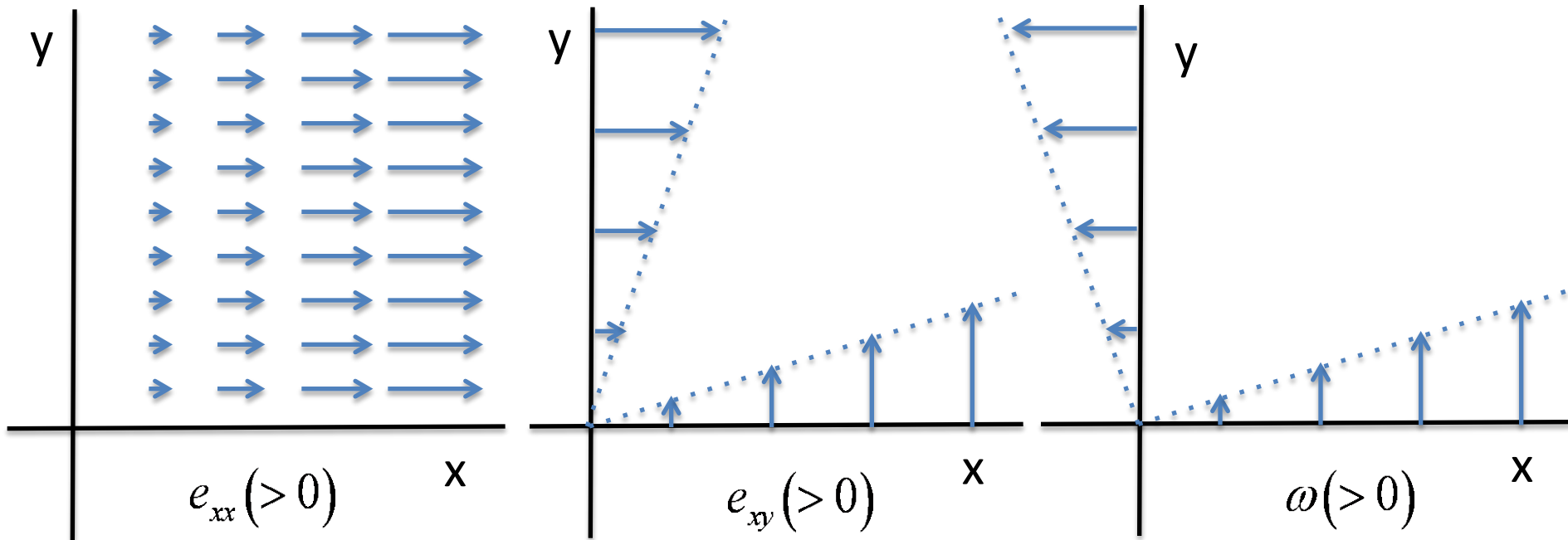
$$\boxed{e_{xx} = \frac{\partial u}{\partial x} \quad e_{yy} = \frac{\partial v}{\partial y} \quad e_{xy} = \frac{1}{2}\left(\frac{\partial u}{\partial y} + \frac{\partial v}{\partial x}\right)}$$

– Rigid rotation

$$\boxed{\omega = \frac{1}{2}\left(\frac{\partial v}{\partial x} - \frac{\partial u}{\partial y}\right)}$$

2.3 Strain and strain rate

- Physical meaning of strain components



“Linear strain”

Denotes length change in the direction or size change of the medium

“Shear strain”

Denotes angle change or shape change of the medium

“rigid rotation”

Denotes counter-clockwise rotation of the medium

2.3 Strain and strain rate

- Linear strain in an arbitrary direction θ

$$e_\theta = dL / L$$

$$x = r \cos \theta \quad y = r \sin \theta$$

$$u_r = u \cos \theta + v \sin \theta \quad u_\theta = -u \sin \theta + v \cos \theta$$

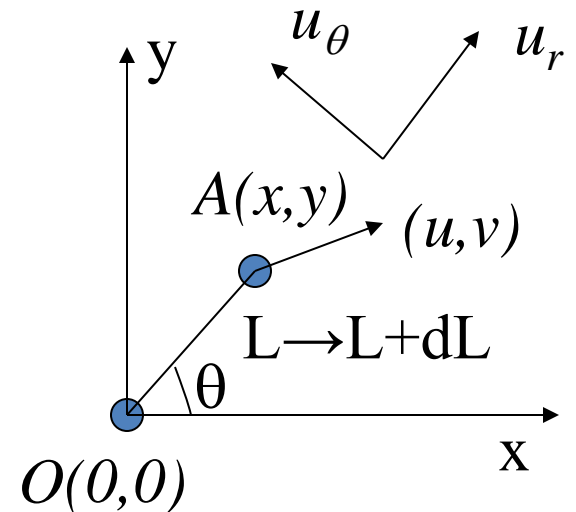
$$e_\theta = \frac{\partial u_r}{\partial r}$$

$$= \left(\frac{\partial x}{\partial r} \frac{\partial}{\partial x} + \frac{\partial y}{\partial r} \frac{\partial}{\partial y} \right) (u \cos \theta + v \sin \theta)$$

$$= \left(\cos \theta \frac{\partial}{\partial x} + \sin \theta \frac{\partial}{\partial y} \right) (u \cos \theta + v \sin \theta)$$

$$= \cos^2 \theta \frac{\partial u}{\partial x} + \sin^2 \theta \frac{\partial v}{\partial y} + \sin \theta \cos \theta \left(\frac{\partial u}{\partial y} + \frac{\partial v}{\partial x} \right)$$

$$= e_{xx} \cos^2 \theta + e_{yy} \sin^2 \theta + e_{xy} \sin 2\theta$$



$$e_\theta = e_{xx} \cos^2 \theta + e_{yy} \sin^2 \theta + e_{xy} \sin 2\theta$$

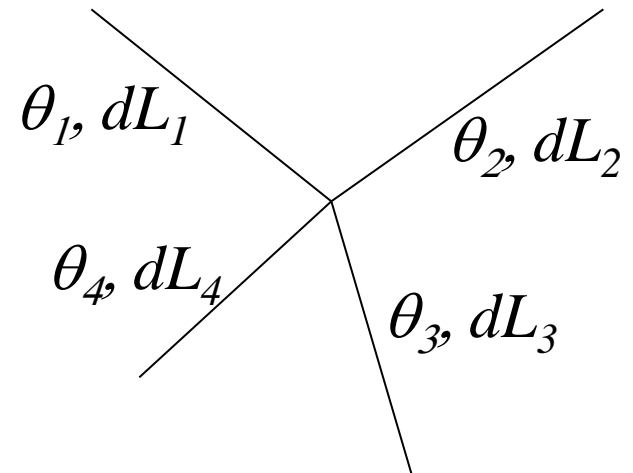
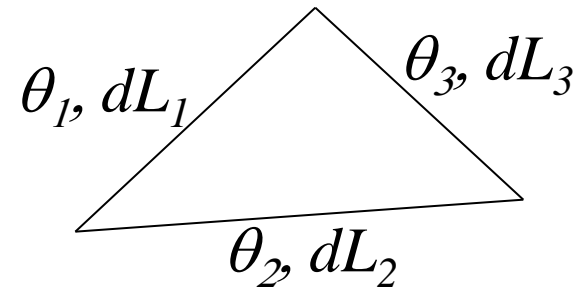
2.3 Strain and strain rate

- Estimation of 2-D strain tensor
 - 3 unknowns (e_{xx} , e_{yy} , e_{xy})
 - More than 3 observations of linear strain
 - Least squares estimation

$$\frac{dL_1}{L_1} = e_{xx} \cos^2 \theta_1 + e_{yy} \sin^2 \theta_1 + e_{xy} \sin 2\theta_1$$

$$\frac{dL_2}{L_2} = e_{xx} \cos^2 \theta_2 + e_{yy} \sin^2 \theta_2 + e_{xy} \sin 2\theta_2$$

$$\frac{dL_3}{L_3} = e_{xx} \cos^2 \theta_3 + e_{yy} \sin^2 \theta_3 + e_{xy} \sin 2\theta_3$$



2.3 Strain and strain rate

- Principal strain
 - Defined as linear strain taking its maximum and minimum values. These two directions are perpendicular each other.
 - In the direction of principal strain, shear strain component becomes zero.
 - Principal strain axes (maximum and minimum values and its direction) fully describes the deformation.

$$e_{\theta} = e_{xx} \cos^2 \theta + e_{yy} \sin^2 \theta + e_{xy} \sin 2\theta$$

$$= \frac{e_{xx} + e_{yy}}{2} + \frac{e_{xx} - e_{yy}}{2} \cos 2\theta + e_{xy} \sin 2\theta$$

$$e_{\theta} = \frac{e_{xx} + e_{yy}}{2} + \sin(\alpha + 2\theta) \sqrt{\frac{(e_{xx} - e_{yy})^2}{4} + e_{xy}^2}$$

$$\frac{\partial e_{\theta}}{\partial \theta} = (e_{yy} - e_{xx}) \sin 2\theta + 2e_{xy} \cos 2\theta = 0$$

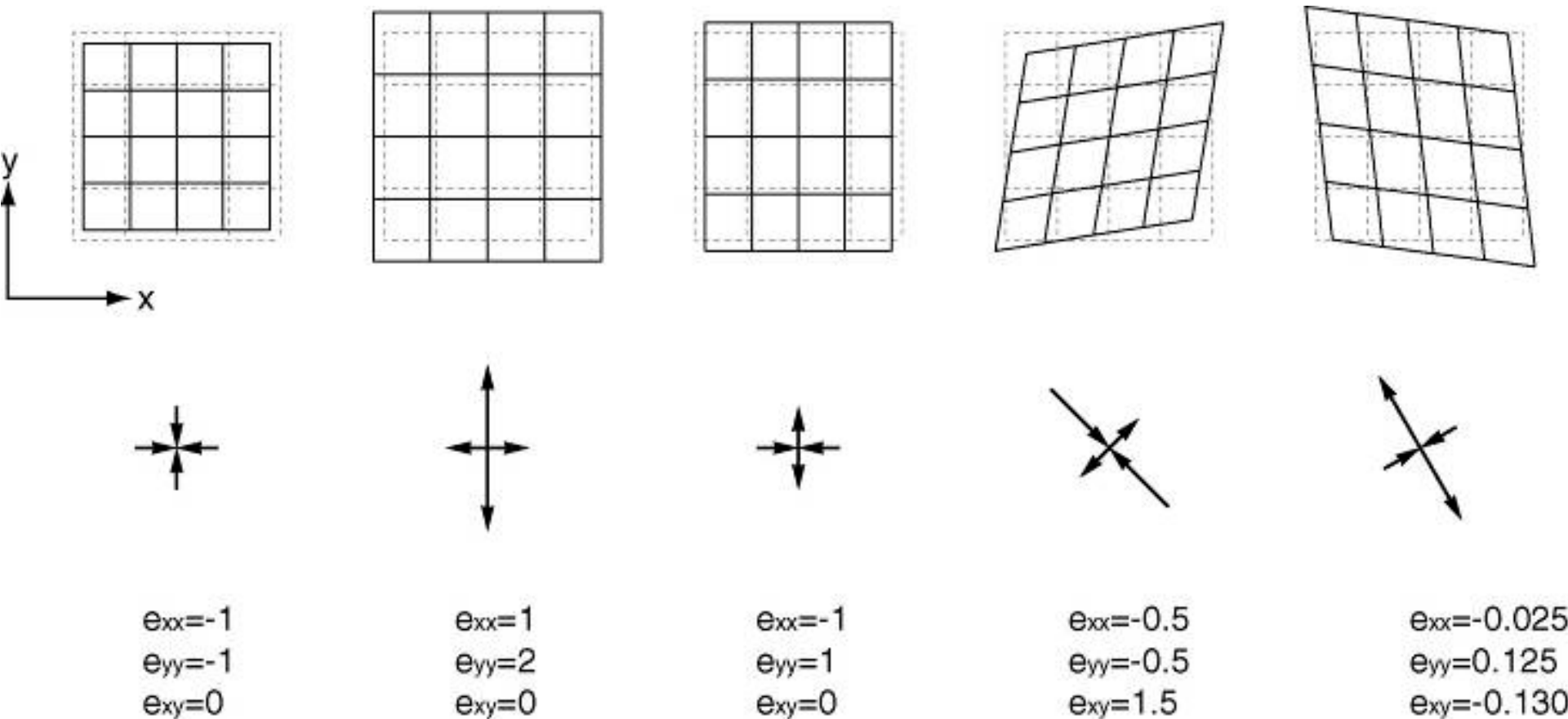
$$\sin \alpha = \frac{e_{xx} - e_{yy}}{\sqrt{(e_{xx} - e_{yy})^2 + 4e_{xy}^2}} \quad \cos \alpha = \frac{2e_{xy}}{\sqrt{(e_{xx} - e_{yy})^2 + 4e_{xy}^2}}$$

$$\tan 2\theta = \frac{2e_{xy}}{e_{xx} - e_{yy}}$$

$$e_{1,2} = \frac{e_{xx} + e_{yy}}{2} \pm \sqrt{\frac{(e_{xx} - e_{yy})^2}{4} + e_{xy}^2}$$

2.3 Strain and strain rate

- Different expression of strain

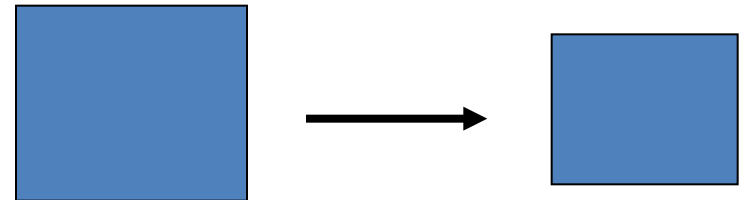


2.3 Strain and strain rate

- Two scalar quantities are frequently used to describe the crustal strain

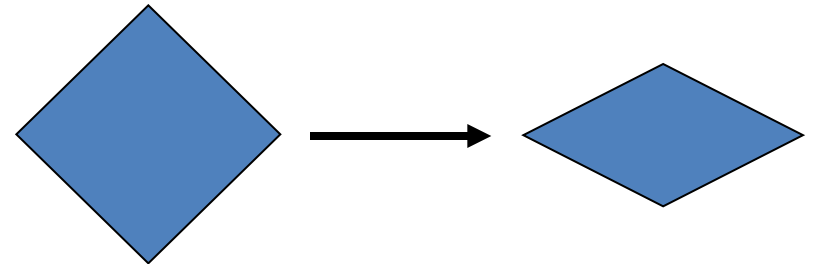
– dilatation:

$$\Delta = e_{xx} + e_{yy} = e_1 + e_2$$



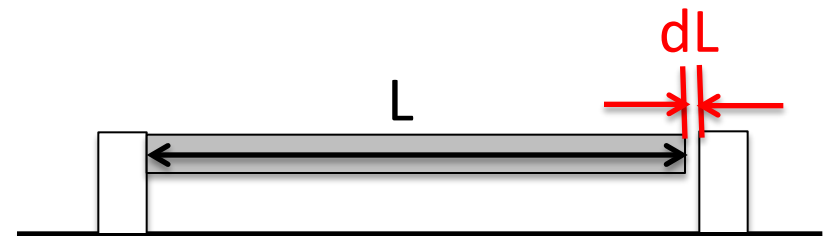
– Maximum shear strain:

$$\Sigma = \sqrt{\frac{(e_{xx} - e_{yy})^2}{4} + e_{xy}^2} = \frac{e_1 - e_2}{2}$$

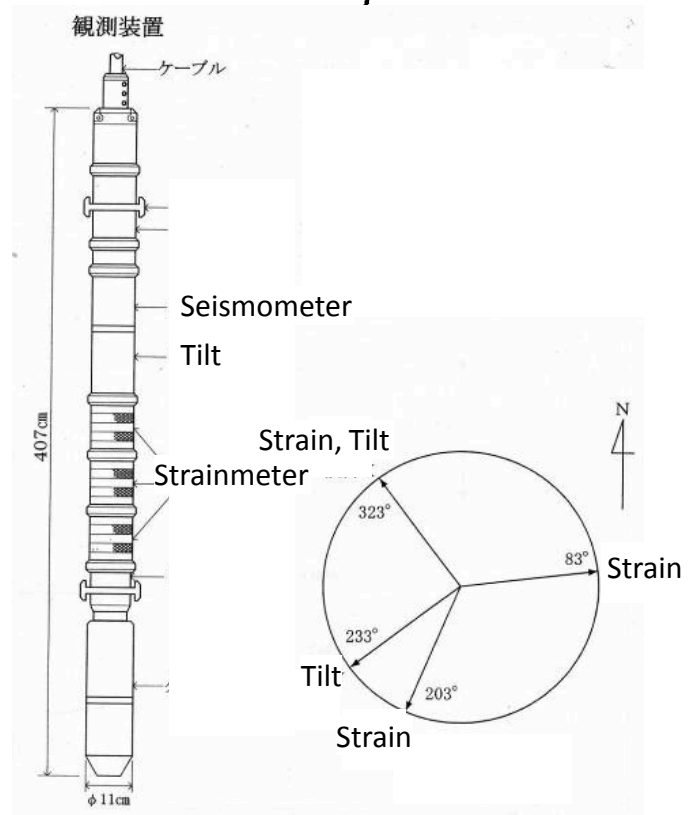


Measurement of strain

- Geodetic survey
 - Triangulation
 - trilateration
 - Continuous GPS array
- Extensometer
 - Measure length change of crystal rod to obtain linear strain
 - Array of extensometers are used to obtain strain tensor
 - Installed in a vault (tunnel)
- Borehole strainmeter
 - Installed in a vertical hole
 - Advanced instrument with a diameter of ~10cm
 - Low noise and high sensitivity



$$e = \frac{dL}{L}$$



Practice

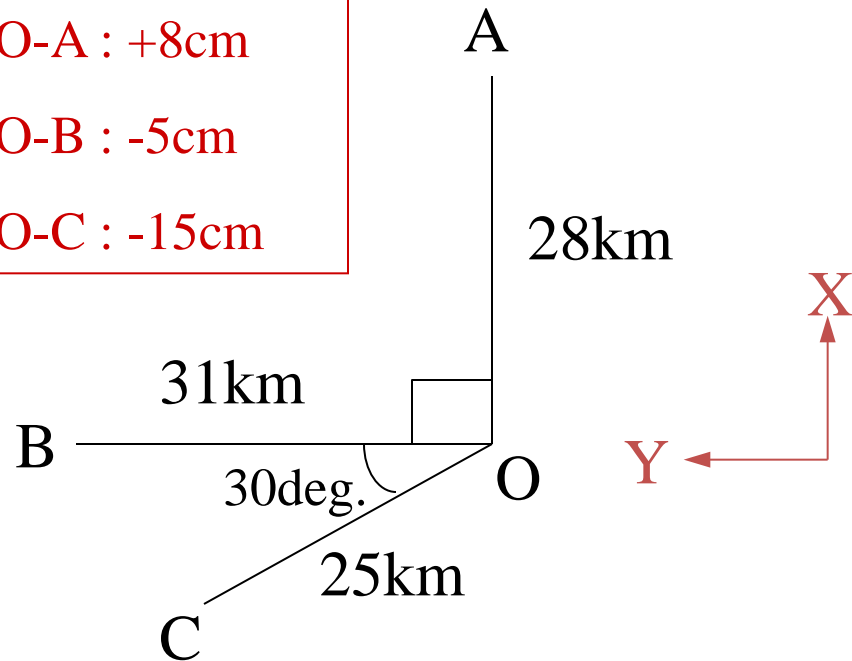
- Calculate strain components
 - e_{xx} , e_{xy} , e_{yy}
- Calculate principal strain rate axes

Length Change

O-A : +8cm

O-B : -5cm

O-C : -15cm



$$e_{yy} = \frac{-5 \times 10^{-2}}{31 \times 10^3} = -1.6 \times 10^{-6}$$

$$e_{xx} = \frac{8 \times 10^{-2}}{28 \times 10^3} = 2.9 \times 10^{-6}$$

$$e_{OC} = \frac{-15 \times 10^{-2}}{25 \times 10^3} = -6.0 \times 10^{-6}$$

Practice: Answer

$$e_{OC} = e_{xx} \cos^2 120^\circ + e_{yy} \sin^2 120^\circ + 2 \times e_{xy} \sin 120^\circ \cos 120^\circ$$

$$e_{xy} = \frac{1}{2} \left(e_{OC} \sec 120^\circ \csc 120^\circ - e_{xx} \cot 120^\circ - e_{yy} \tan 120^\circ \right)$$

$$e_{xy} = \frac{1}{2} \left\{ -6.0 \times \frac{2}{\sqrt{3}} \times (-2) - 2.9 \times \left(-\frac{1}{\sqrt{3}} \right) - (-1.6) \times \left(-\sqrt{3} \right) \right\} \times 10^{-6}$$

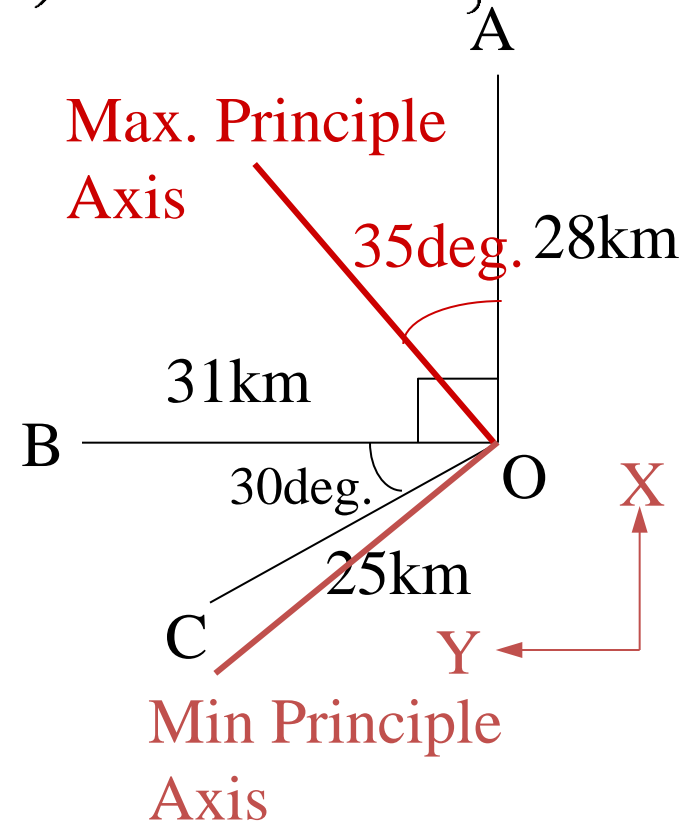
$$e_{xy} = 6.4 \times 10^{-6}$$

$$\tan 2\theta = \frac{2e_{xy}}{e_{xx} - e_{yy}} = \frac{2 \times 6.4}{2.9 - (-1.6)} = 2.8$$

$$\theta = 35^\circ$$

$$e_1 = 7.4 \times 10^{-6}$$

$$e_2 = -6.1 \times 10^{-6}$$



2.4. Tilt

- Tilt is differential uplift at the ground surface resulting slope change.
- There are two types of measurement of tilt:
 - Surface measurement

- Leveling, water-tube, bubble

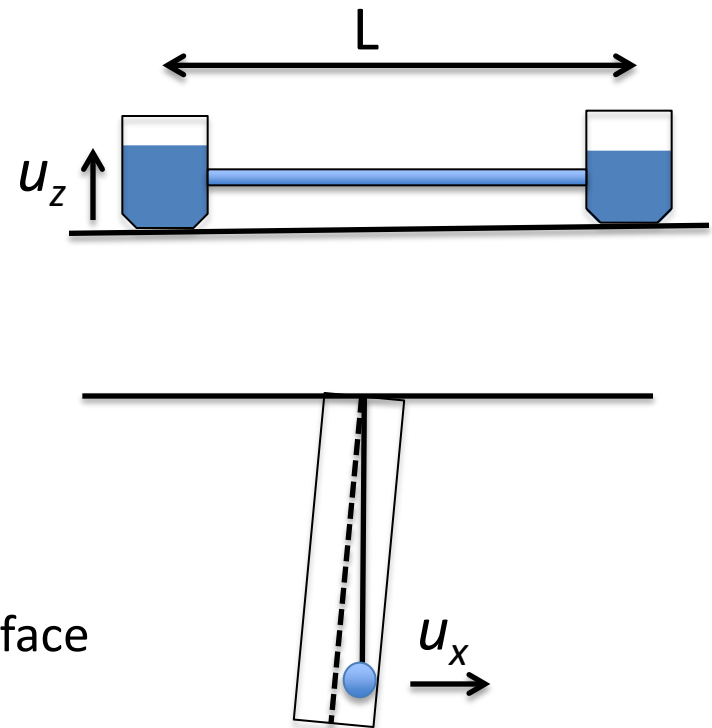
$$t_x = \frac{\partial u_z}{\partial x} \quad t_y = \frac{\partial u_z}{\partial y}$$

- Borehole measurement

- Pendulum

$$t'_x = \frac{\partial u_x}{\partial z} = -t_x \quad t'_y = \frac{\partial u_y}{\partial z} = -t_y$$

Two measurements are equivalent under free surface ($\tau_{zx} = \tau_{xz} = 0$) condition.



2.5. Stress and strain

- Relationship between stress and strain defines mechanical property of the medium and is called **constitutive equation**.

– Elastic solid

$$\tau_{ij} = \lambda e_{kk} \delta_{ij} + 2\mu e_{ij}$$

λ, μ : Lamé's constant

(μ : rigidity, $K = \lambda + 2\mu/3$: bulk modulus)

– Viscous fluid

$$\tau_{ij} = -p\delta_{ij} + 2\eta\dot{e}_{ij}$$

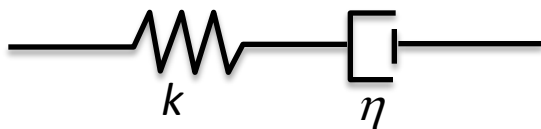
η : viscosity

2.5. Stress and strain

- Viscoelasticity

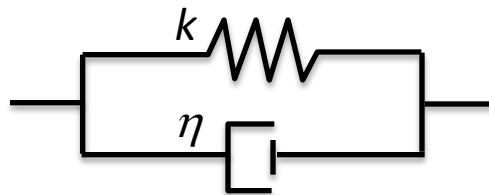
- A large part of the Earth, such as the mantle and the lower crust, exhibits viscoelastic behavior. These parts respond elastically in a short (seismological) time scale, but they flow in a long (geological) time scale.

Maxwell model



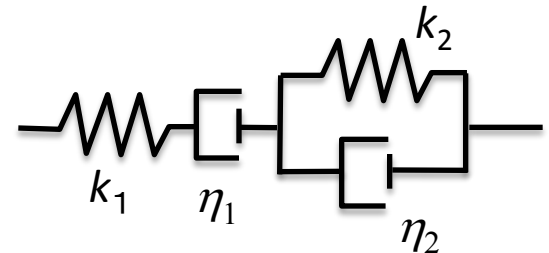
$$\frac{\dot{\tau}}{k} + \frac{\tau}{\eta} = \dot{\epsilon}$$

Kelvin (Voigt) model



$$\tau = k\epsilon + \eta\dot{\epsilon}$$

Burgers model



$$2\eta_2\ddot{\epsilon} + 2k_2\dot{\epsilon} = \frac{\eta_2}{k_1}\ddot{\tau} + \left(\frac{\eta_2}{\eta_1} + \frac{k_2}{k_1} + 1\right)\dot{\tau} + \frac{k_2}{\eta_1}\tau$$

2.5 Stress and strain

- In the Earth, viscous flow relax shear stress, but normal stress is not relaxed at all. In such a sense, volumetric deformation (related to bulk modulus K) is elastic, while shear deformation (related to shear modulus μ) is viscoelastic.
- The constitutive equation is written as follows.

$$\dot{\tau}_{ij} + \frac{\mu}{\eta} \left(\tau_{ij} - \frac{1}{3} \tau_{kk} \delta_{ij} \right) = \lambda \dot{\epsilon}_{kk} \delta_{ij} + 2\mu \dot{\epsilon}_{ij}$$

2.5 Stress and strain

- Nonlinear rheology
 - Viscous behavior of the mantle is caused by either **diffusion creep** or **dislocation creep** of minerals.
 - Constitutive equation of viscous flow is nonlinear in general, and is represented by the following Arrhenius law with power law dependence on stress.

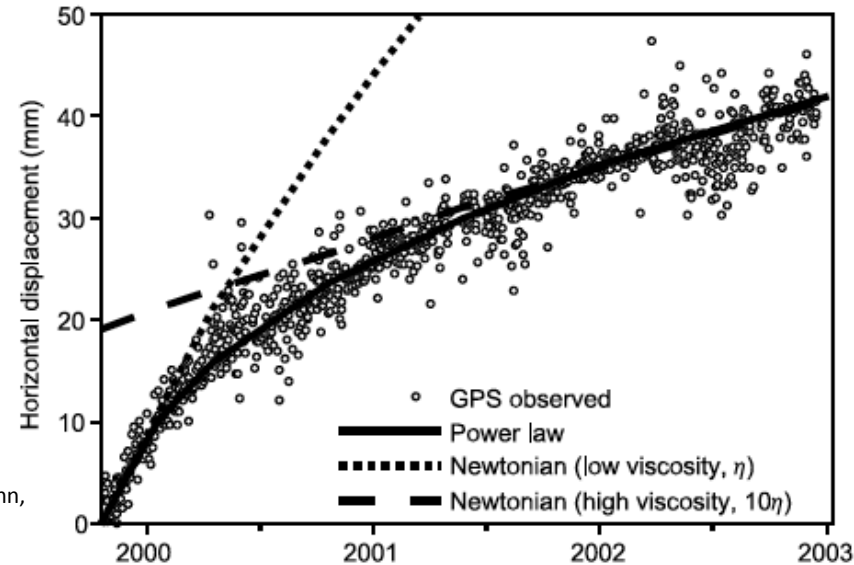
$$\dot{\epsilon} = A_0 \sigma^n \exp\left(-\frac{H^*}{RT}\right)$$

- Such a behavior is called “**power law creep**”, which is highly temperature dependent.
- Apparent viscosity decrease exponentially with the temperature, facilitating mantle flow at depth.
- There are studies reporting detection of power law creep behavior in postseismic deformation.

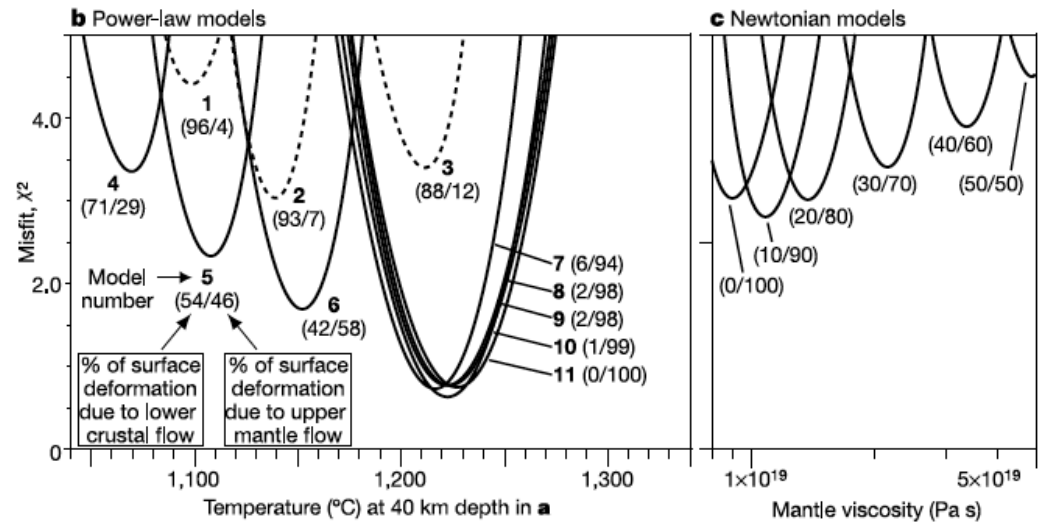
Power law rheology

- Based on postseismic deformation of the 1999 Hector Mine earthquake in California, Freed and Burgmann (2004, Nature) demonstrated that the power law creep explains the transient feature of GPS data and estimated candidate composition of the crust and the mantle.

(Permission from Macmillann Publishers Ltd: Nature, "Evidence of Power-law Flow in the Mojave Desert Mantle", Freed and Burgmann, 2004.)



Model number	Crust	Mantle
1	wet quartzite 1	dry olivine
2	dry quartzite 1	dry olivine
3	dry quartzite 2	dry olivine
4	wet quartzite 1	wet olivine
5	dry quartzite 1	wet olivine
6	dry quartzite 2	wet olivine
7	quartz-diorite	wet olivine
8	aplite	wet olivine
9	wet quartzite 2	wet olivine
10	anorthosite	wet olivine
11	diabase	wet olivine

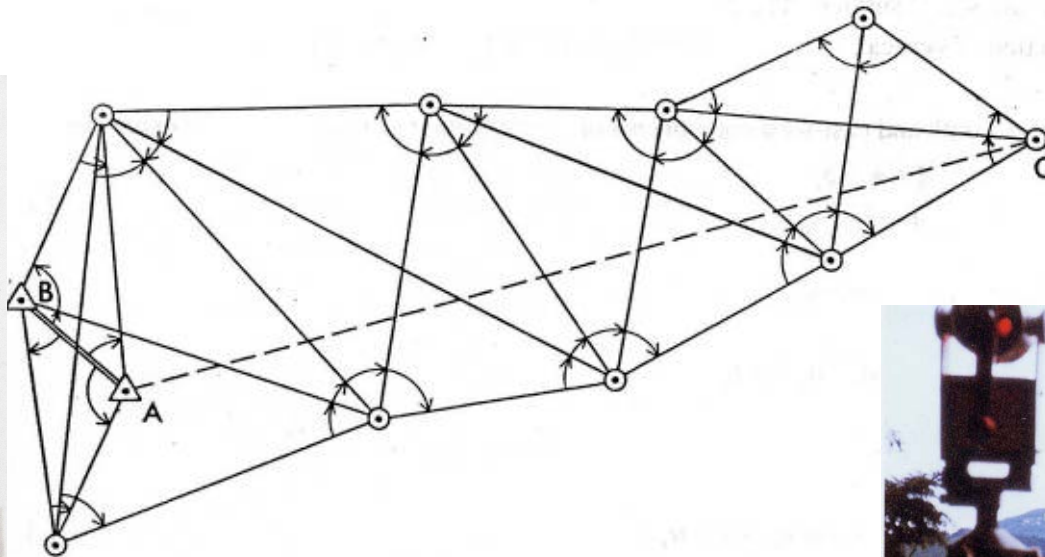


3. Observation methods

- Geodetic survey
 - Triangulation/trilateration
 - Leveling
- Continuous observation
 - Strain/tilt
 - Tide gauges
- Space geodetic techniques
 - GNSS (GPS, GLONASS, ...)
 - Synthetic aperture radar (SAR)

3.1 Triangulation/trilateration

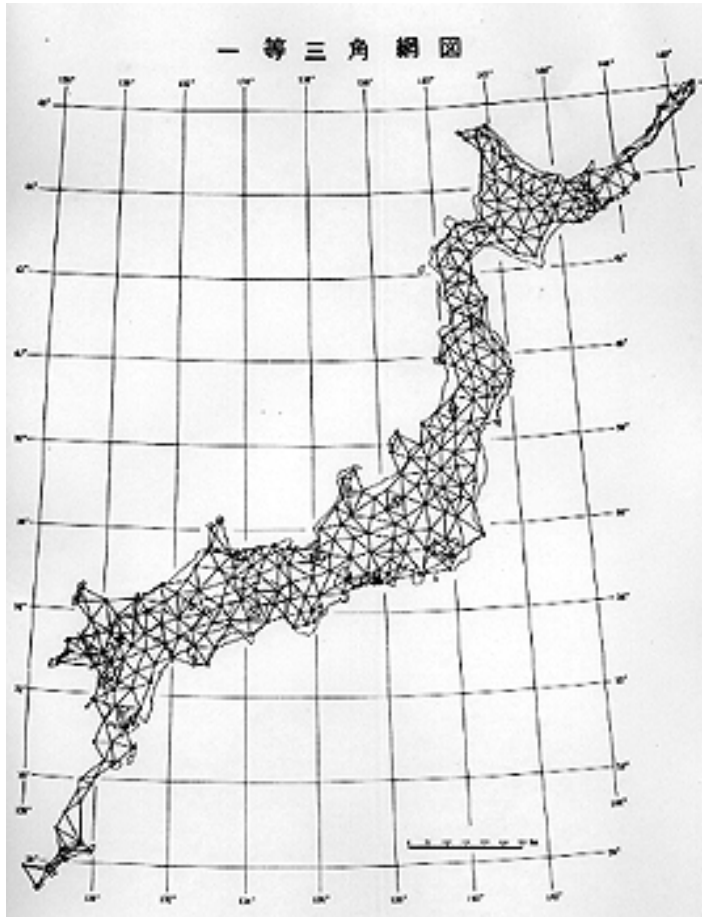
- Triangulation is a conventional survey method to define horizontal control point network.
- To define horizontal coordinates of benchmarks based on measurements of angles and side lengths.
- Even for triangulation, direct measurement of baseline lengths is necessary.
- Redundant observation is required for robust processing .
- There remains a degree of freedom about rigid rotation of the network



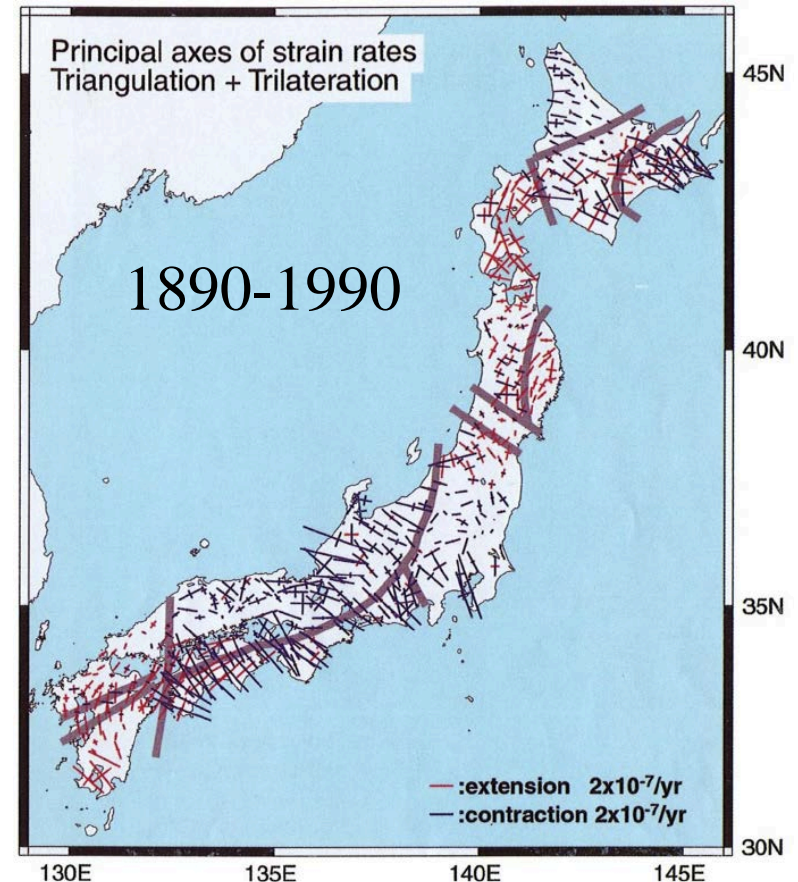
IISSE



3.1 Triangulation/trilateration



(GSI Website :
<http://www.gsi.go.jp/MUSEUM/TOKUBE/KIKA5-sanka111.htm>)



(“Average Horizontal Crustal Strain Rates in Japan during Interseismic Period Deduced from Geodetic Surveys (Part2)”, Ishikawa and Hashimoto, 1999, The Seismological Society of Japan)

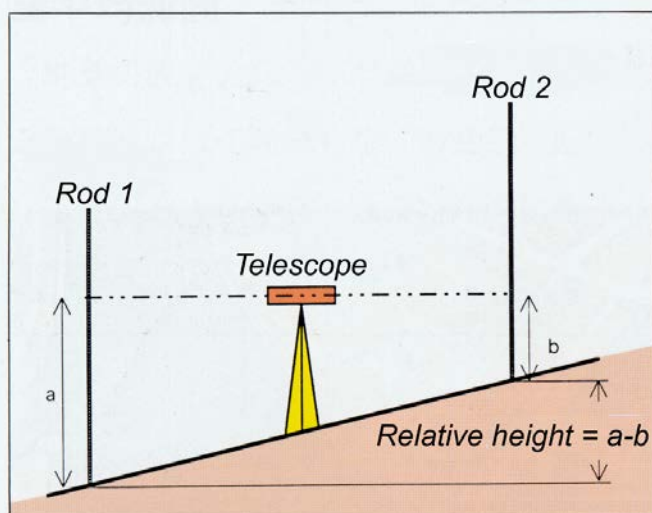
- The Japanese triangulation network was constructed in the late 19th century and has been resurveyed several times to reveal crustal deformation of the Japan Islands.

3.2 Leveling

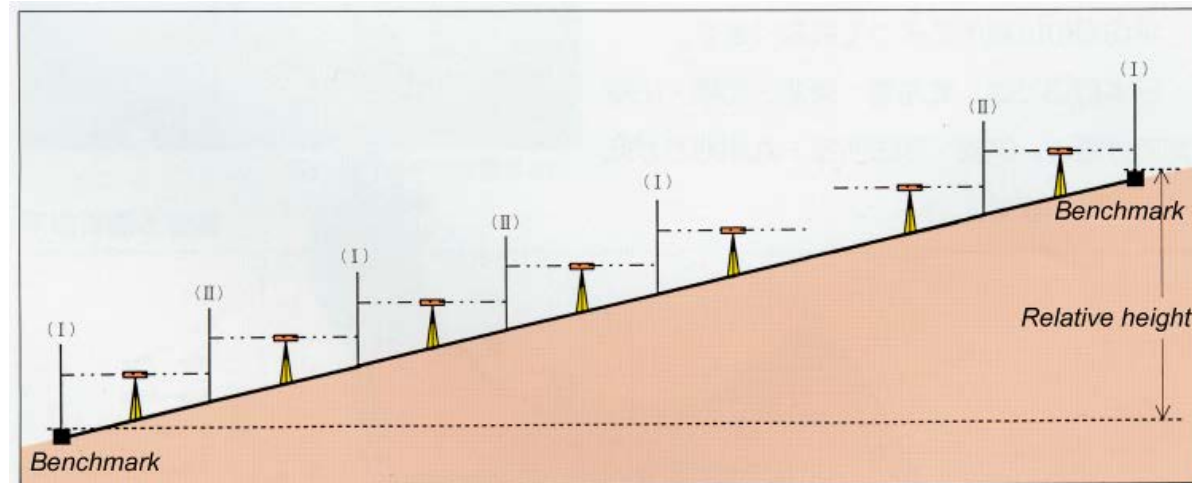
- Leveling survey is conducted to measure height of benchmarks.
- Reading of leveling rods is repeated to obtain cumulative relative heights between benchmarks.
- Obtained height refers to the mean sea level (geoid) and should be distinguished from the ellipsoidal height.
- Leveling has the highest precision about vertical displacement.



(All pictures from GSI Website : <http://vldb.gsi.go.jp/sokuchi/level/survey.html>)



2013.2.17/18

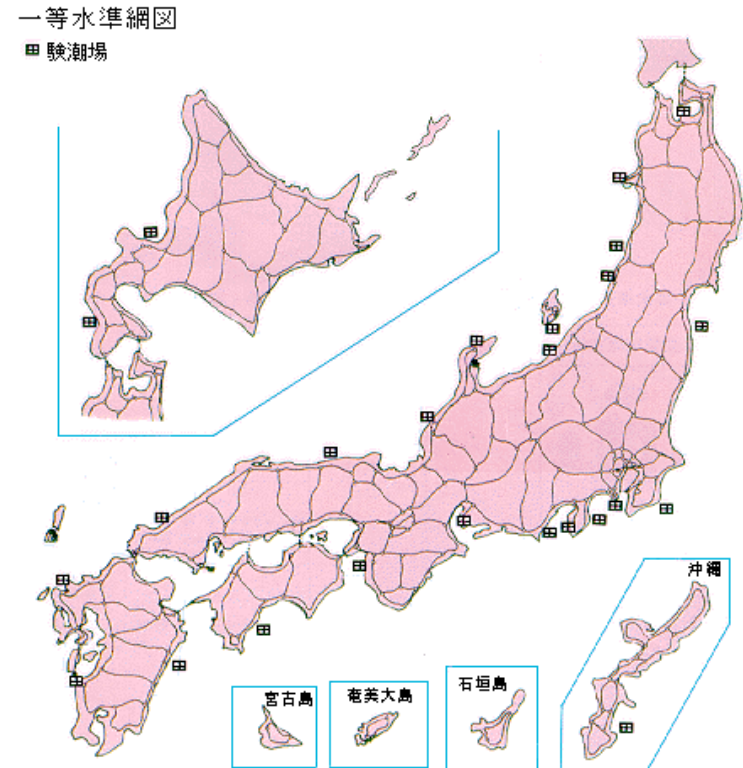


IISEE

45

3.2 Leveling

- Japanese leveling network was also constructed in the late 19th century, and has been resurveyed every 10 years.
- Leveling has revealed various tectonic deformation related to earthquakes



(GSI Website: <http://vldb.gsi.go.jp/sokuchi/level/point.html>)

3.3 Tidal observation

- Tidal observation is multi-purpose
 - Define mean sea level as the reference of vertical datum
 - Monitor vertical movement of coastal area
 - Monitor global sea level change
 - Monitor high tide and tsunami
- Long history
 - Some tide gauges have been operated more than 100 years

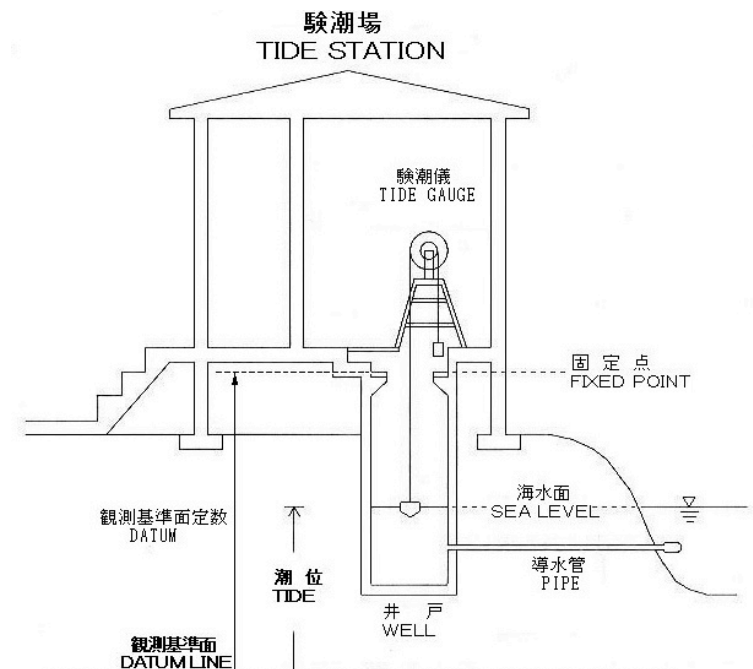
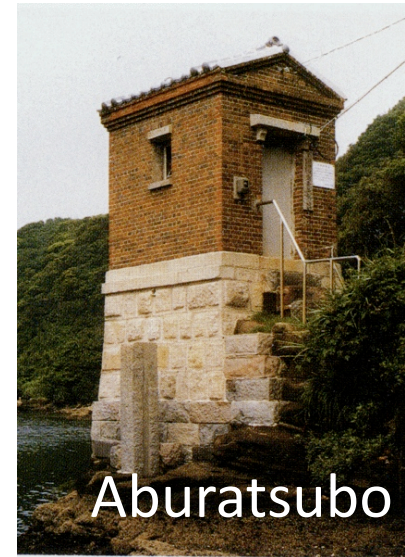
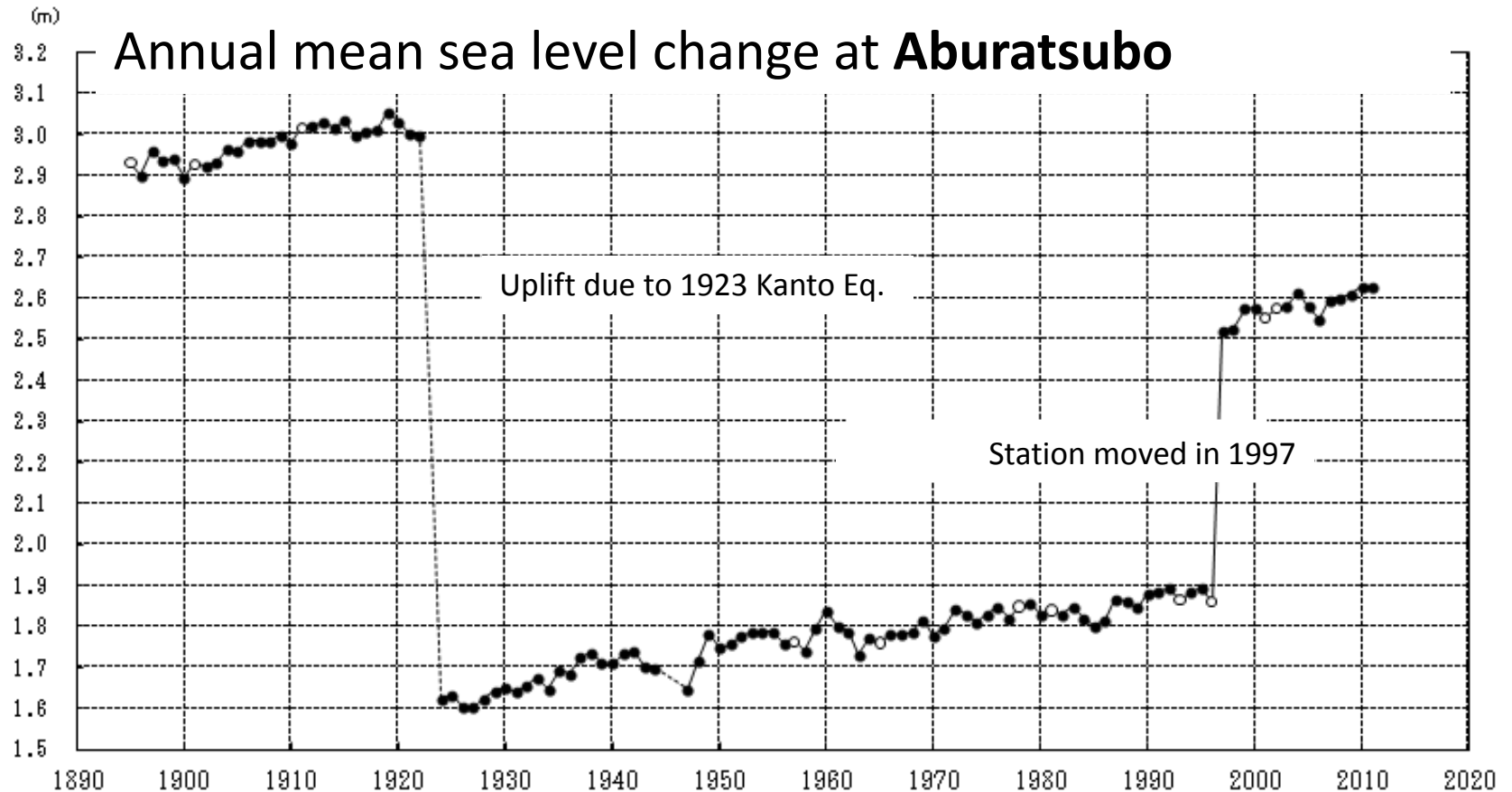


(Photo and figure from GSI Website :
<http://tide.gsi.go.jp/st/1/old1.jpg>
<http://tide.gsi.go.jp/comment.html>)

3.3 Tidal observation



(GSI Website :
<http://cais.gsi.go.jp/cmdc/center/kentyoujo/aburatubo/aburatubo.html>)

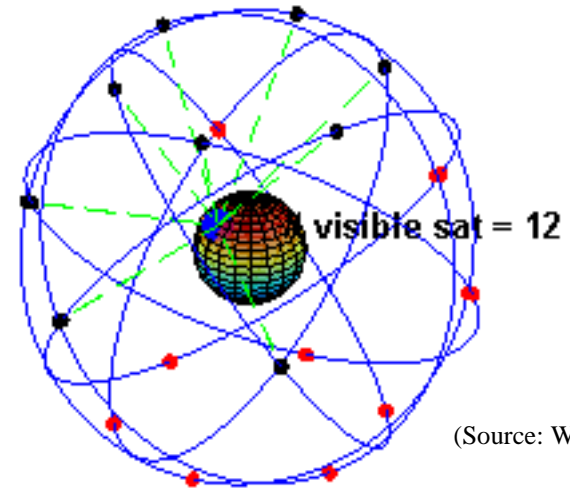
Detected coseismic uplift as well as interseismic subsidence.

3.4. GNSS

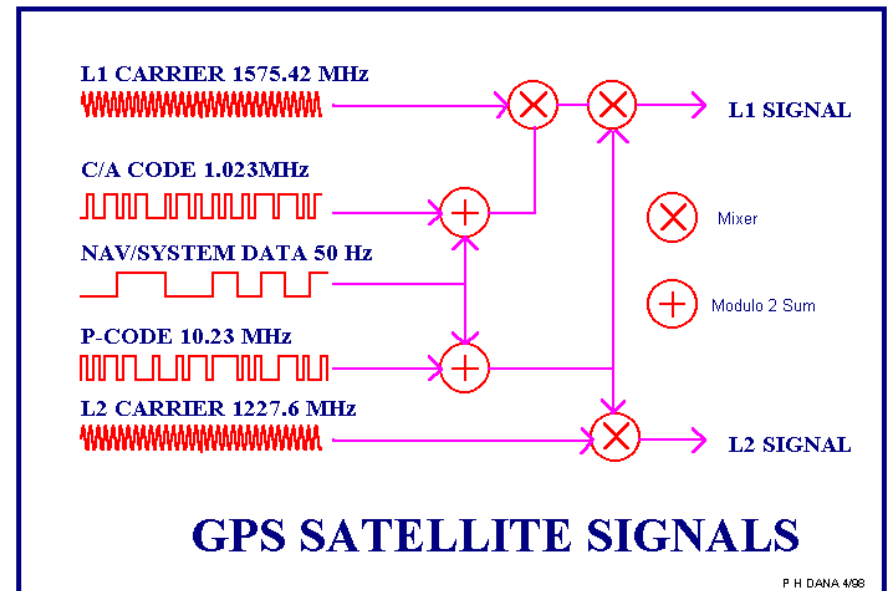
- Global Navigation Satellite System
 - Artificial satellite system designed for navigation and surveying purposes
- GPS (Global Positioning System): USA
- GLONASS: Russia
- Galileo: EU
- Compass: China
- QZSS: Japan (Michibiki)

3.4 GNSS: GPS

- 24 satellites on 6 orbits
- Code (C/A, P) : binary signals used for navigation
 - C/A-code: 1.023MHz
 - P-code: 10.23MHz
 - P-code information is limited for military use
- Carrier phase (L1, L2): sinusoidal signal used for precise surveying
 - L1: 1575.42MHz (19.0cm)
 - L2: 1227.60MHz (24.4cm)



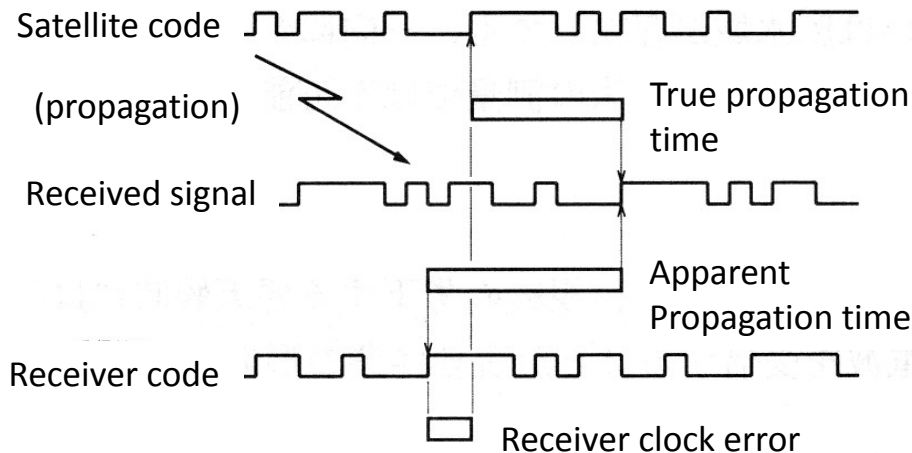
(Source: Wikipedia)



(Peter H. Dana, Department of Geography, University of Texas at Austin: http://www.colorado.edu/geography/gcraft/notes/gps/gps_f.html)

3.4. GNSS: GPS

- Point positioning
 - 1) extract code data from received signal
 - 2) generate the code data within the receiver
 - 3) Compare (1) and (2) : difference = propagation time + clock error
 - 4) Satellite orbit can be extracted from code data.
 - 5) Solve 4 or more simultaneous equations
 - 6) Antenna position and time are estimated



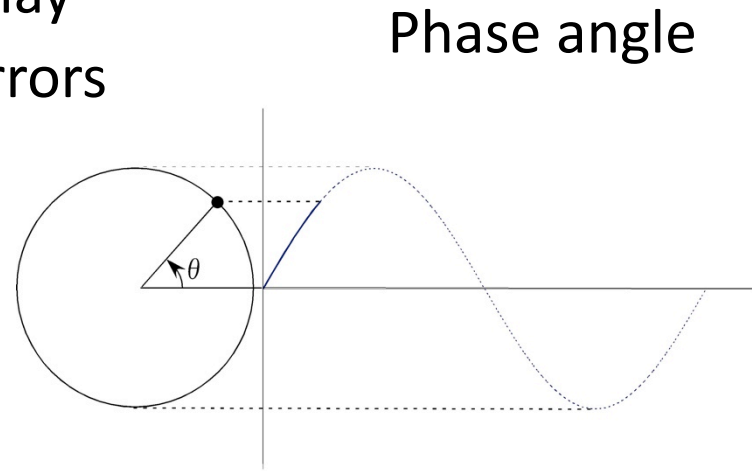
$$\begin{cases} \sqrt{(x_1 - X)^2 + (y_1 - Y)^2 + (z_1 - Z)^2} = c(t_1 + \Delta t) \\ \sqrt{(x_2 - X)^2 + (y_2 - Y)^2 + (z_2 - Z)^2} = c(t_2 + \Delta t) \\ \sqrt{(x_3 - X)^2 + (y_3 - Y)^2 + (z_3 - Z)^2} = c(t_3 + \Delta t) \\ \sqrt{(x_4 - X)^2 + (y_4 - Y)^2 + (z_4 - Z)^2} = c(t_4 + \Delta t) \end{cases}$$

Satellite position: (x,y,z) , propagation time: t ,

Antenna position : (X,Y,Z) , Receiver clock error: Δt , Speed of light: c

3.4. GNSS: GPS

- Relative positioning
 - Carrier phase measurement
 - Wavelength: $\sim 20\text{cm}$
 - 1 degree phase angle: $\sim 0.5\text{mm}$
 - Estimation of integer ambiguity
 - Number of waves between satellite and antenna
 - Estimation of tropospheric delay
 - Estimation of satellite clock errors



3.4. GNSS: GPS

- Pseudo-range: distance between a satellite and a receiving antenna without correction of clock errors

- Code pseudorange: point positioning

$$\begin{aligned} R &= c(t_R - t^S) = c\left\{(t_R(GPS) + \delta_R) - (t^S(GPS) + \delta^S)\right\} \\ &= c\{\Delta t(GPS) + \Delta\delta\} = \rho + c\Delta\delta \end{aligned}$$

- Phase pseudorange: relative positioning

$$\begin{aligned} \lambda\Phi_i^j(t) &= \rho_i^j(t) + \lambda N_i^j + c\{\delta^j(t) - \delta_i(t)\} + \lambda\{\Delta_{ion}(t) + \Delta_{trop}(t)\} \\ \rho_i^j(t) &= \sqrt{(x^j - x_i)^2 + (y^j - y_i)^2 + (z^j - z_i)^2} \end{aligned}$$

λ : wavelength, f : frequency, ρ : distance between receiver and satellite
 N_i^j : phase ambiguity(integer), δ^j : satellite clock offset, δ_i : receiver clock offset
 Δ_{ion} : ionospheric delay, Δ_{trp} : tropospheric delay

RINEX file

header

```
2.10 OBSERVATION DATA G (GPS) RINEX VERSION / TYPE
teqc 2004Jan13 gpsops 20050102 00:02:04UTCPGM / RUN BY / DATE
30.0000 INTERVAL
1 1 WAVELENGTH FACT L1/2
7 L1 L2 P1 P2 C1 S1 S2 # / TYPES OF OBSERV
Linux 2.0.36|Pentium II|gcc -static|Linux|486/DX+ COMMENT
soc2rnx ver 1.15 gpsops 2-Jan-2005 00:02:02 COMMENT
S1, if present, is the SNR for the C/A data stream on L1. COMMENT
SNR is mapped to RINEX snr flag value [1,4-9] COMMENT
SNR: >316 >100 >31.6 >10 >3.2 >0 bad=0 COMMENT
L1 & L2: 9 8 7 6 5 4 1 COMMENT
COMMENT
This data is provided as a public service by NASA/JPL. COMMENT
No warranty is expressed or implied regarding suitability COMMENT
for use. For further information, contact: COMMENT
Dave Stowers, NASA/JPL m/s 238-600 COMMENT
4800 Oak Grove Drive, Pasadena CA 91109 USA COMMENT
COMMENT
Forced Modulo Decimation to 30 seconds COMMENT
2005 1 1 0 0 0.0000000 GPS TIME OF FIRST OBS
GGN JPL OBSERVER / AGENCY
121 AOAD/M_T JPLA ANT # / TYPE
-3855263.0267 3427432.5484 3741020.3254 APPROX POSITION XYZ
-0.0350 0.0000 0.0000 ANTENNA: DELTA H/E/N
LP020002603 ASHTECH Z-XII3 CD00 1s soc2rnx REC # / TYPE / VERS
USUD MARKER NAME
21729S007 MARKER NUMBER
END OF HEADER
```

Observation data

```
05 1 1 0 0 0.0000000 0 9G 1G16G23G25G 6G21G 3G15G14
114701971.93848 89378144.27948 21827071.8914 21827076.5514 21827072.0324
233.000 190.000
109608906.09448 85409526.58348 20857888.6944 20857891.5294 20857889.4984
243.000 212.000
119955190.78648 93471569.59948 22826720.2824 22826720.3684 22826720.1424
225.000 171.000
108089384.38448 84225479.13348 20568737.7004 20568740.8544 20568737.9854
249.000 221.000
121994536.12348 95060651.98448 23214808.8714 23214811.9154 23214808.8884
222.000 169.000
124786324.12448 97236083.57748 23746059.4264 23746062.3074 23746060.3804
220.000 161.000
119987184.85848 93496492.70548 22832812.8944 22832818.3714 22832813.9684
221.000 170.000
130169178.97948 101430505.77348 24770389.2074 24770395.8984 24770391.2604
214.000 151.000
131635059.33748 102572747.58348 25049339.2814 25049349.1024 25049339.4774
192.000 131.000
JPLA Training Course 0.0000000 0 9G 1G16G23G25G 6G21G 3G15G14 54
114785012.56048 89442851.21248 21842874.5014 21842878.7804 21842874.5794
235.000 188.000
```

3.4. GNSS(GPS)

Combination of observables to eliminate clock offset

- Single difference

$$\Phi_{AB}^j(t) = \rho_{AB}^j(t) / \lambda + N_{AB}^j - f\delta_{AB}(t)$$

$$\rho_{AB}^j(t) = \rho_B^j(t) - \rho_A^j(t)$$

$$N_{AB}^j = N_B^j - N_A^j$$

$$\delta_{AB}(t) = \delta_B(t) - \delta_A(t)$$

– elimination of
satellite clock offset

- Double difference

$$\Phi_{AB}^{jk}(t) = \rho_{AB}^{jk}(t) / \lambda + N_{AB}^{jk}$$

$$\begin{aligned} \rho_{AB}^{jk}(t) &= \rho_{AB}^k(t) - \rho_{AB}^j(t) \\ &= \rho_B^k(t) - \rho_A^k(t) - \rho_B^j(t) + \rho_A^j(t) \end{aligned}$$

$$\begin{aligned} N_{AB}^{jk} &= N_{AB}^k - N_{AB}^j \\ &= N_B^k - N_A^k - N_B^j + N_A^j \end{aligned}$$

– elimination of
receiver clock offset

Precise measurement of GPS

- Static measurement (relative positioning)
 - Analyze phase data for 1-24 hours to estimate single coordinate
 - Requires a reference site to cancel satellite clock error
 - Construct baselines and create double difference observables
 - Daily coordinate has mm-level precision
 - Precision deteriorates for shorter observation period.
- Precise point positioning (PPP)
 - Analyze phase data from a single site
 - Fast and efficient calculation
 - Needs satellite clock information from outer sources
- Kinematic measurement
 - Epoch-by-epoch estimate of station coordinate
 - Continuous satellite tracking and ambiguity fixing are necessary
 - Precision depends on the baseline length
 - Real-time analysis (RTK) is now becoming popular recently with an improving accuracy of predicted satellite orbits

3.4. GNSS(GPS)

- Errors in GPS results
 - Satellite orbit/clock
 - Post-processing
 - Prediction
 - Ionospheric perturbation
 - Can be corrected using multi-frequency data
 - Troposphere
 - The most serious error source. Up to a few cm.
 - Site-specific error: maybe important at volcanoes
 - Monument instability
 - Multi-path

3.4. GNSS: Analysis software (1)

- Commercial software
 - Spider (Leica): http://www.leica-geosystems.com/en/Leica-GNSS-Spider_83498.htm
 - 4D control (Trimble): <http://www.trimble.com/survey/trimble4dcontrol.aspx>
 - Giodis (Javad): <http://www.javad.com/jgnss/products/software/giodis.html>
- Merit
 - GUI
 - Easy to use
 - System Integration from data acquisition to monitoring
- Demerit
 - Cost
 - Black box : impossible to understand the algorithm, no modification

3.4. GNSS: Analysis software (2)

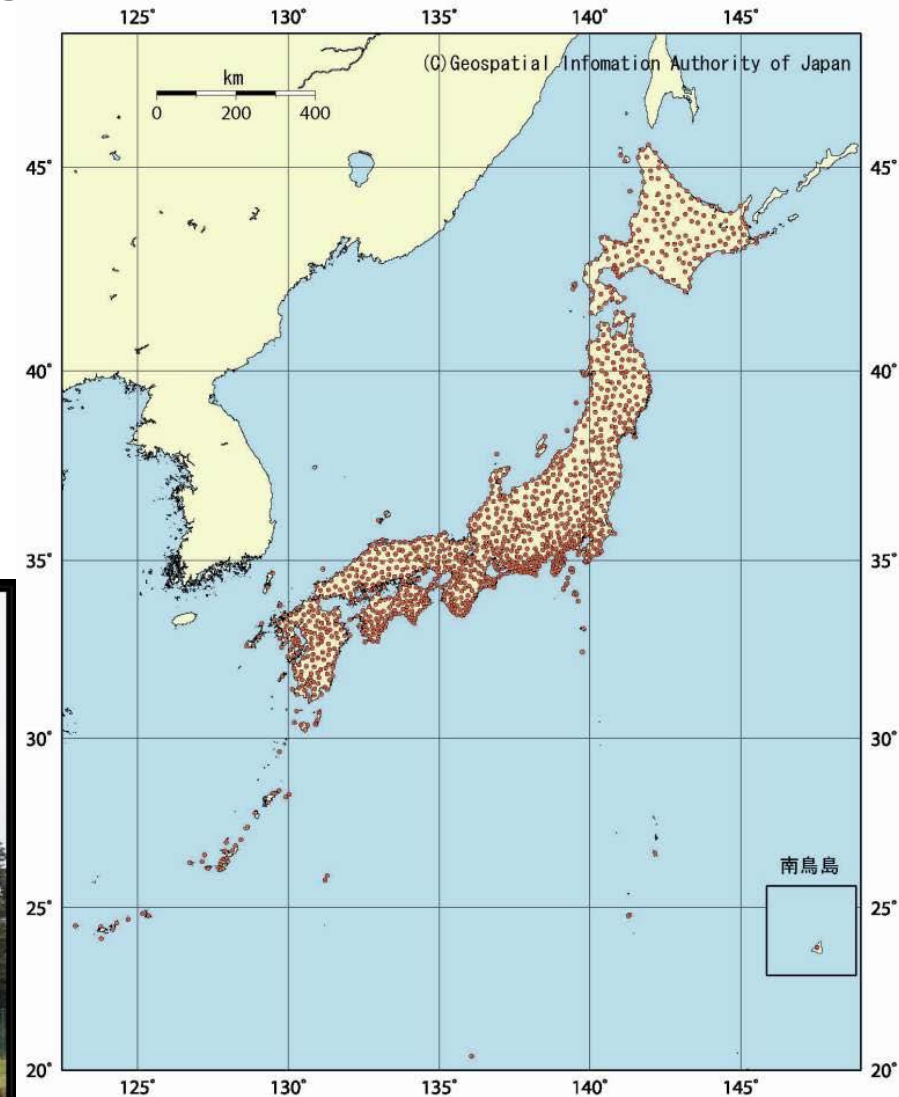
- Scientific software
 - GAMIT/GLOBK : <http://bowie.mit.edu/>
 - Gipsy: <https://gipsy-oasis.jpl.nasa.gov/>
 - Bernese: <http://www.bernese.unibe.ch/>
 - RTKLIB: <http://www.rtklib.com/>
- Merits
 - Cost (basically free, Bernese costs CHF12000)
 - Open source (except for Gipsy)
 - Flexibility
 - State-of-the-art technology
- Demerits
 - Needs specialist knowledge and training
 - Graphical interface is not included (except for RTKLIB)

3.4. GNSS: Information sources

- IGS (international GNSS Service):
<http://igscb.jpl.nasa.gov/>
 - Global monitoring network (station logs, observation data, etc.)
 - Satellite orbit and earth rotation parameters
- UNAVCO: <http://www.unavco.org/>
 - TEQC software: Data preprocessing
- ITRF: <http://itrf.ensg.ign.fr/>
 - Definition of International terrestrial reference frame and site coordinate/velocity

3.4. GNSS: Japanese GPS Network

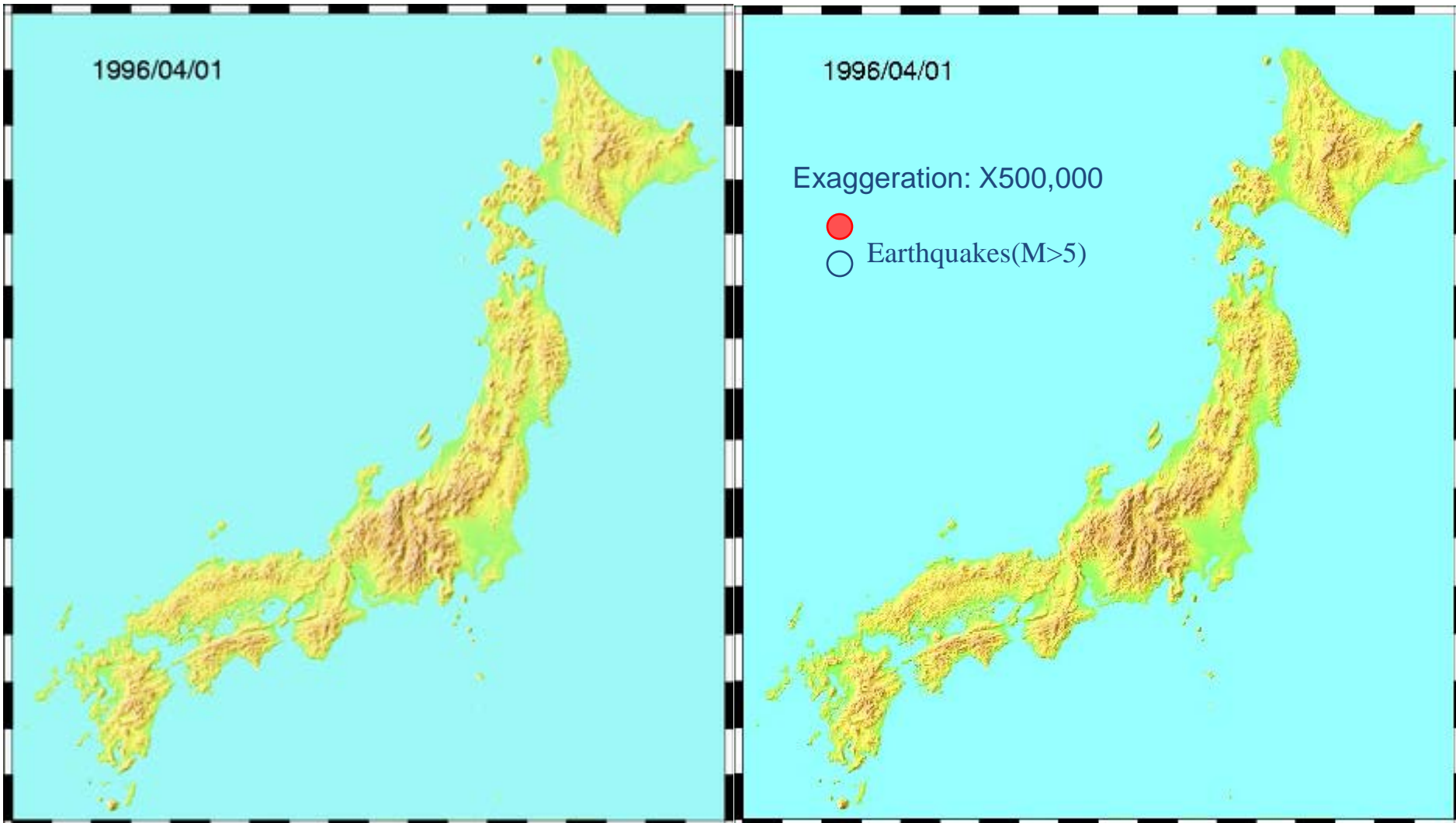
- Operated by G.S.I.
- GEONET (GPS Earth Observation NETwork)
- Operated since 1994
- About 1200 stations
- All the stations are operated 24hrs., 365days/yr



(All figures from GSI Website:
http://terras.gsi.go.jp/gps/gps-based_control_station.html)

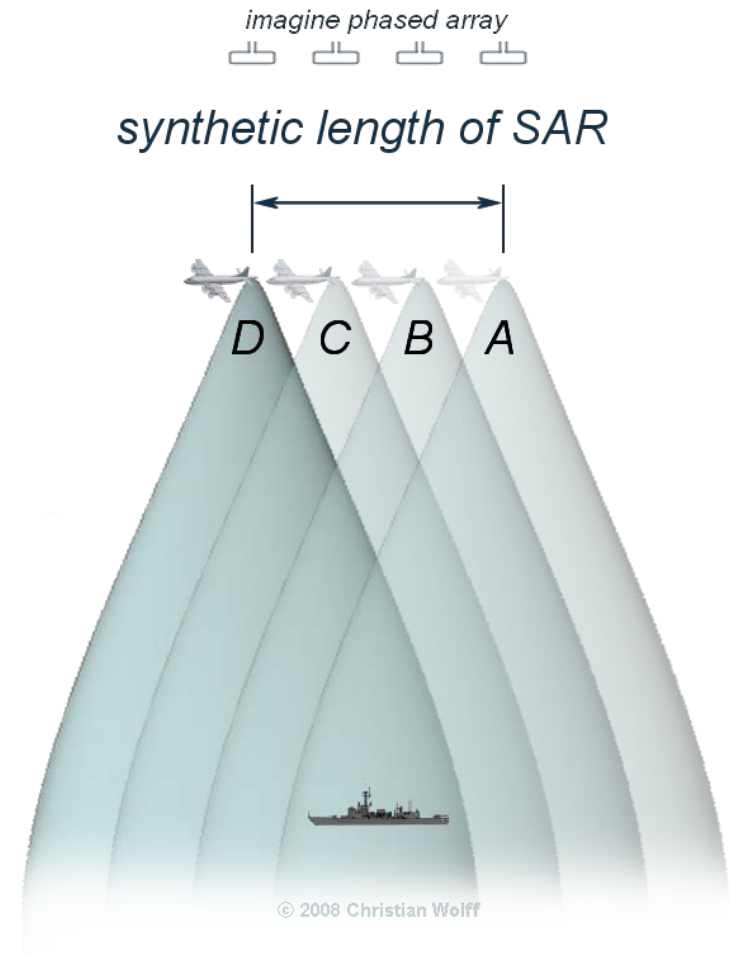


Crustal deformation of Japan as viewed by GPS



3.5. Interferometry SAR

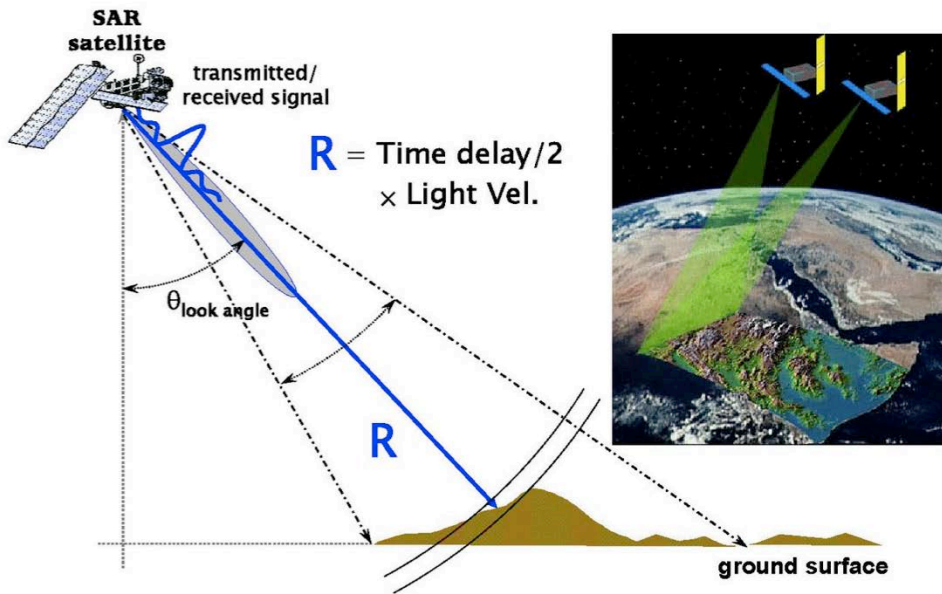
- Synthetic aperture radar
 - Side-looking radar system mounted on satellites and airplanes
 - Multiple images taken in accordance with the flight are synthesized to simulate a large aperture phased array realizing a high resolution image of the target.



(This figure is published under the licenses of GNU Free Documentation License and Creative Commons License: www.radartutorial.eu/)

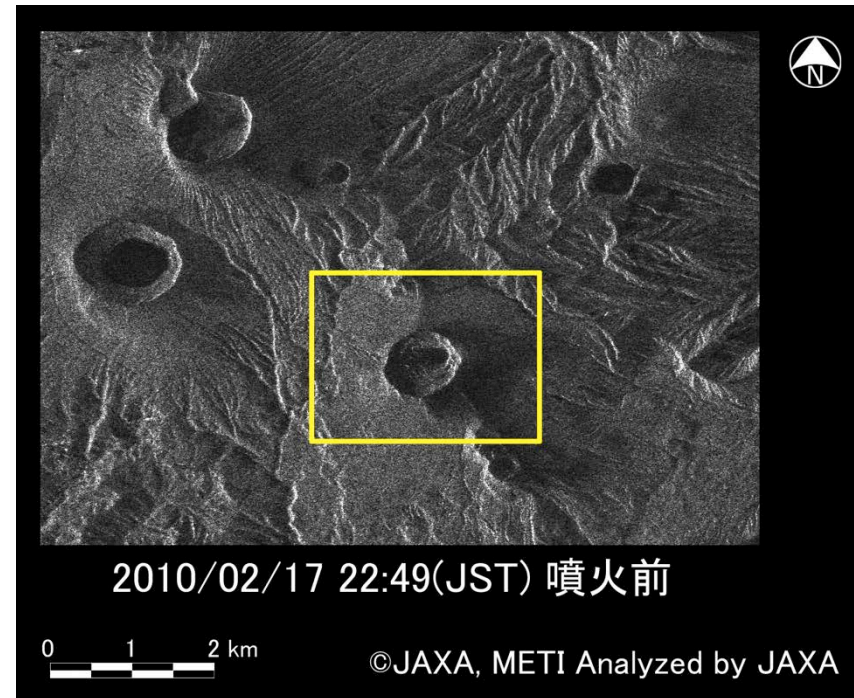
3.5. Interferometry SAR

Principle of SAR imaging



(University of South Florida,
Website: <http://labs.cas.usf.edu/geodesy/sar.html>)

Example of SAR image

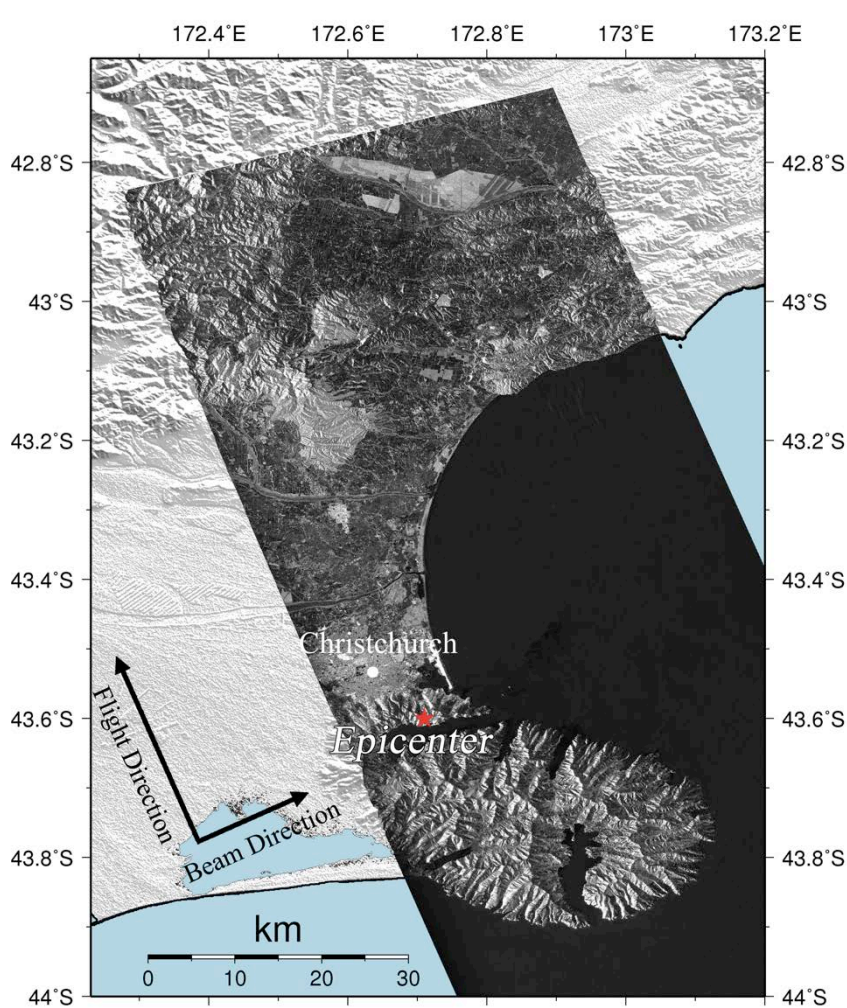


3.5. Interferometry SAR

- Interferometry
 - By matching two images taken at different times, phase change pattern is estimated
 - Detect LOS (line-of sight) distance change (1-dimensional)

3.5. Interferometry SAR

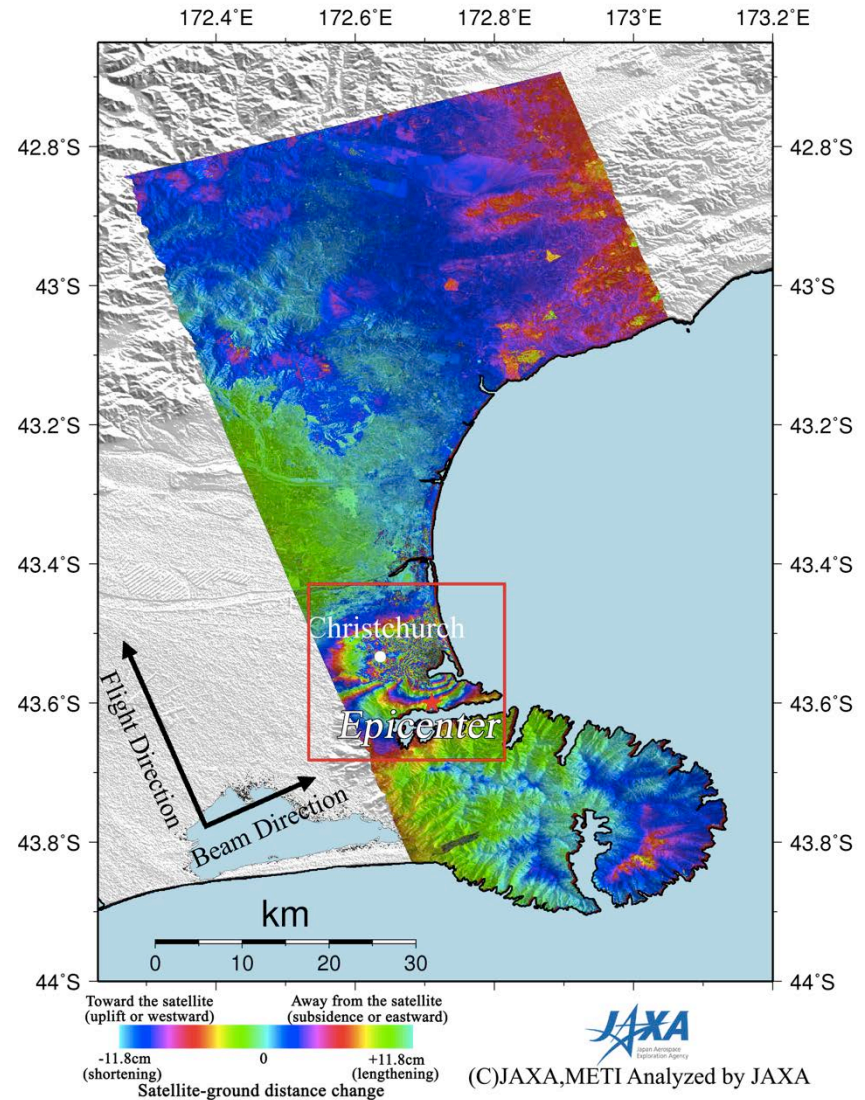
- Example: 2011 Christchurch earthquake



Amplitude image


(C)JAXA,METI Analyzed by JAXA

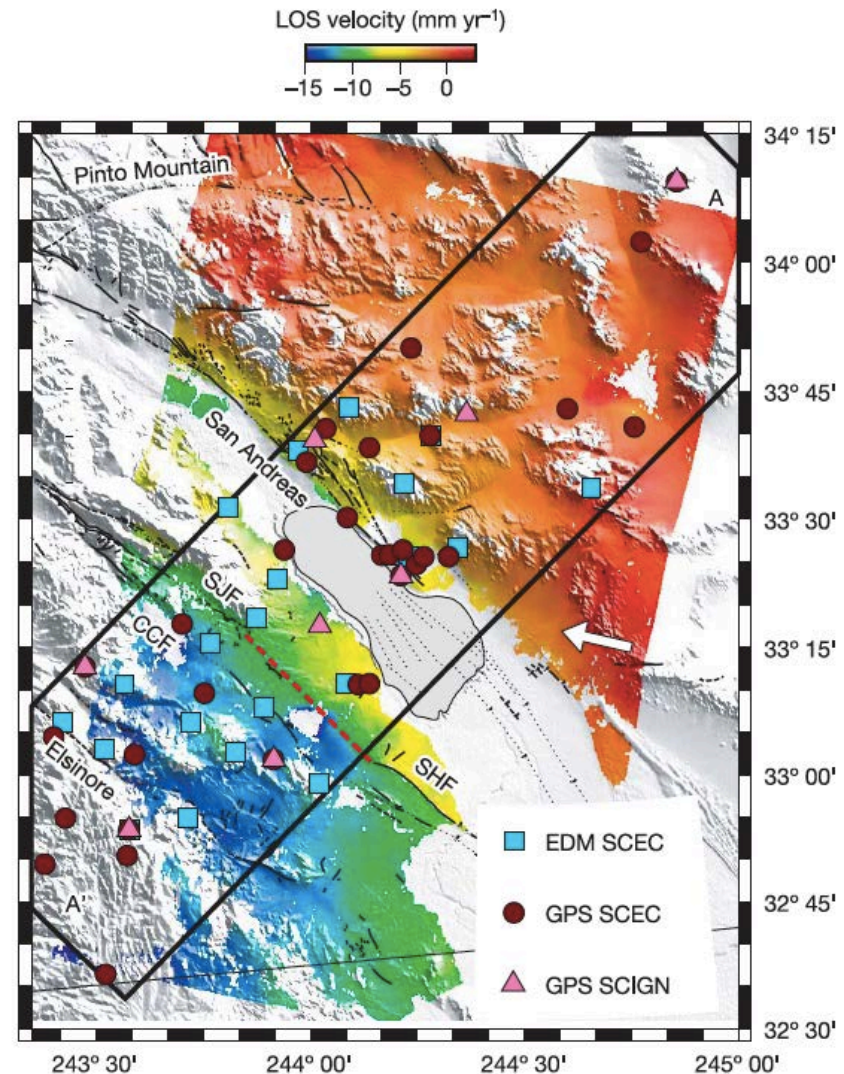
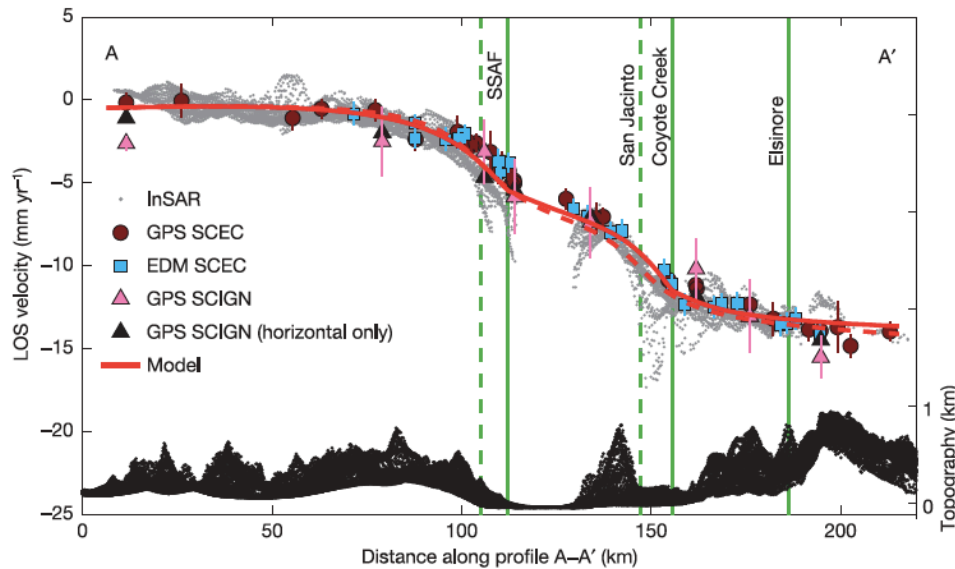
IISSE



(C)JAXA,METI Analyzed by JAXA

3.5. Interferometry SAR

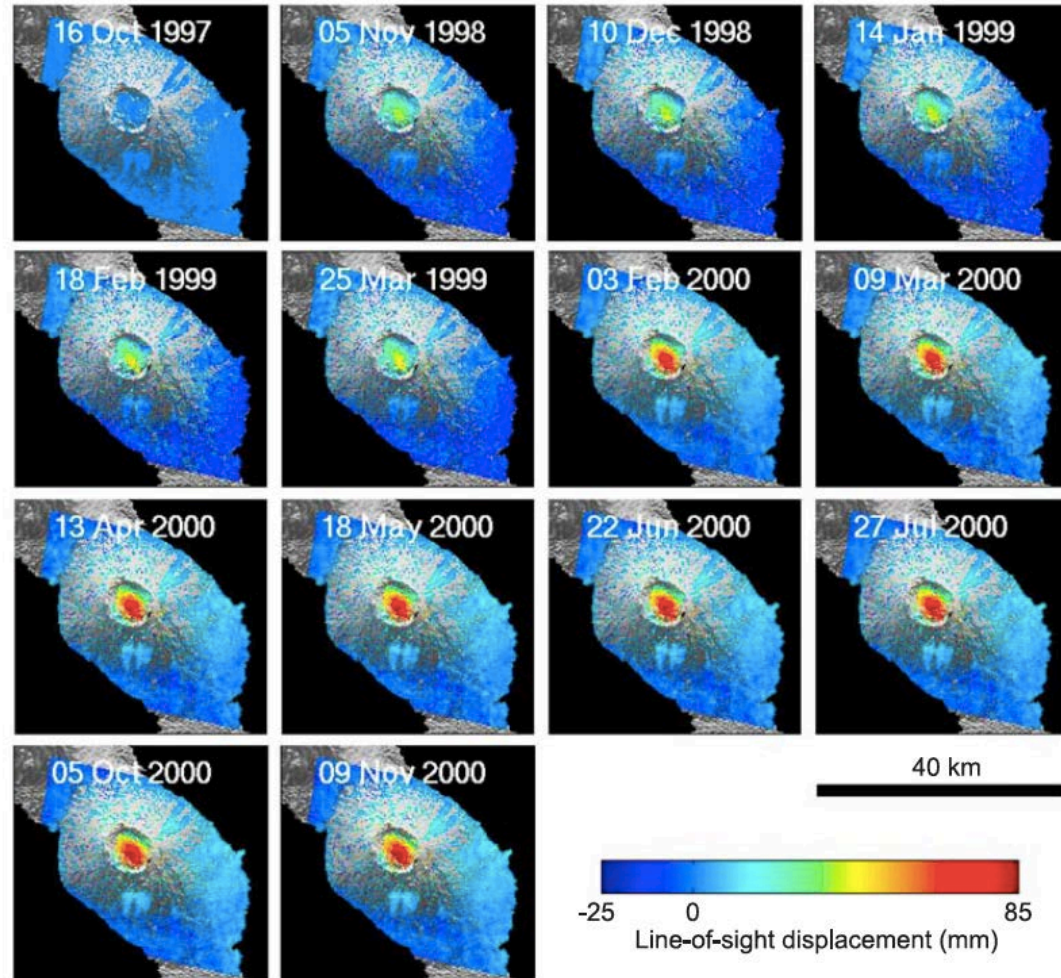
- Southern California
- Detection of interseismic deformation pattern by stacking 35 images
- Height spatial resolution and high accuracy (1-2mm/yr)



(Permission from Macmillann Publishers Ltd: Nature, "Interseismic Strain Accumulation and the Earthquake Potential on the Southern San Andreas Fault System", Yuri Fialko, 2006)

3.5. Interferometry SAR

- Persistent scatterer analysis
- Identify strong scatterers on the ground from multiple images and use them as “benchmarks”
- Time series analysis become possible



(Hooper et al., “Persistent scatterer interferometric synthetic aperture radar for crustal deformation analysis, with application to Volcán Alcedo, Galápagos”
Journal of Geophysical Research: Solid Earth (1978-2012), 112, B7, AGU, 2007.)

3.5. Interferometry SAR

- Satellite
 - L-band ($\lambda \sim 24\text{cm}$): JERS-1(1992-1998), ALOS/PALSAR(2006-2011), ALOS2(2013-)
 - C-band ($\lambda \sim 6\text{cm}$): ERS-1 (1991-2000), ERS-2 (1995-2011), ENVISAT (2002-2012), RADARSAT-1(1995-), RADARSAT-2 (2007-)
 - X-band ($\lambda \sim 3\text{cm}$): TerraSAR-X (2007-), COSMO-SkyMed (2007-)
- Airplane
 - UAVSAR (L-band)
- L-band: good coherency, low resolution, large ionospheric noise
- C(X)-band: poor coherency, high resolution, small ionospheric noise

